European Journal of Medicinal Chemistry 58 (2012) 84–97

Contents lists available at SciVerse ScienceDirect

European Journal of Medicinal Chemistry

journal homepage: http://www.elsevier.com/locate/ejmech

Original article

Design, synthesis and biological evaluation of benzo[*e*][1,2,4]triazin-7(1*H*)-one and [1,2,4]-triazino[5,6,1-*jk*]carbazol-6-one derivatives as dual inhibitors of beta-amyloid aggregation and acetyl/butyryl cholinesterase

Marco Catto [a], Andrey A. Berezin [b], Daniele Lo Re [b], Georgia Loizou [b], Marina Demetriades [b], Angelo De Stradis [c], Francesco Campagna [a], Panayiotis A. Koutentis [b], Angelo Carotti [a,*]

[a] *Dipartimento di Farmacia, Università degli Studi di Bari "Aldo Moro", Via Orabona 4, 70125 Bari, Italy*
[b] *Department of Chemistry, University of Cyprus, PO Box 20537, 1678 Nicosia, Cyprus*
[c] *Istituto di Virologia Vegetale del CNR, Università degli Studi di Bari "Aldo Moro", Via Amendola 165/A, 70126 Bari, Italy*

ARTICLE INFO

Article history:
Received 23 July 2012
Received in revised form
27 September 2012
Accepted 3 October 2012
Available online 11 October 2012

Keywords:
Benzotriazinones
Triazafluoranthenones
Alzheimer's disease
β-Amyloid aggregation inhibitors
Cholinesterase inhibitors
Multitarget-directed ligands

ABSTRACT

Alzheimer's disease (AD) onset and progression are associated with the dysregulation of multiple and complex physiological processes and a successful therapeutic approach should therefore address more than one target. Two new chemical entities, the easily accessible heterocyclic scaffolds 1,3-diphenylbenzo[*e*][1,2,4]triazin-7(1*H*)-one (benzotriazinone **I**) and 2-phenyl-6*H*-[1,2,4]triazino[5,6,1-*jk*]carbazol-6-one (triazafluoranthenone **II**), were explored for their multitarget-directed inhibition of beta-amyloid (Aβ) fibrillization and acetyl- (AChE) and/or butyryl- (BChE) cholinesterase, three valuable targets for AD therapy. Introduction of appropriate amine substituents at positions 6 and 5 on scaffold **I** and **II**, respectively, allowed the preparation of a series of compounds that were tested as $A\beta_{1-40}$ aggregation and cholinesterase inhibitors. Potent inhibitors of Aβ self-aggregation were discovered and among them benzotriazinone **7** exhibited an outstanding IC_{50} equal to 0.37 μM. Compounds bearing a basic amine linked to the heterocyclic scaffold through a linear alkyl chain of varying length also afforded good ChE inhibitors. In particular, benzotriazinone **24** and triazafluoranthenone **38** were endowed with an interesting multiple activity, the former displaying IC_{50} values of 1.4, 1.5 and 1.9 μM on Aβ aggregation and AChE and BChE inhibition, respectively, and the latter showing IC_{50} values of 1.4 and an outstanding 0.025 μM in the Aβ aggregation and BChE inhibition, respectively. Benzotriazinone **24** and triazafluoranthenone **29**, selected owing to their suitable aqueous solubility and Aβ aggregation inhibition, were submitted to a time course kinetic assay followed with thioflavin T (ThT) spectrofluorimetry, circular dichroism (CD) and transmission electron microscopy (TEM). Experimental data indicated that **24** acted at a low concentration ratio (10 μM **24** *vs.* 50 μM Aβ), stabilizing the unstructured Aβ peptide and inhibiting fibrillogenesis, and that **29** also acted as fibrillization inhibitor, but likely enhancing and stabilizing the β-sheet arrangement of Aβ to yield protofibrillar species as detected by TEM.

1. Introduction

Neurodegenerative diseases (NDs) are, along with cancer and cardiovascular diseases, the most important cause of illness and death in developed countries. The high social and clinical costs of healthcare and (familiar) assistance for ND suffering patients [1] are exasperated by the lack of disease-modifying therapies. Despite the wide efforts of both academic and industrial researchers, there are still only a few pharmacological treatments for NDs.

Alzheimer's disease (AD) is by far the most common form of senile dementia, affecting almost ten million people only in Europe [2]. Along with many other NDs, AD is a typical multifactorial disease and its insurgence and progression may be caused by the dysregulation of multiple pathophysiological processes [3], and by environmental [4] and genetic factors [5]. The hallmark of AD is the neuronal degeneration in selected areas of the brain, caused either by overproduction and accumulation of beta amyloid peptide (Aβ) in extracellular aggregates (neuritic plaques), and intracellular formation of neurofibrillary tangles, constituted mainly by hyperphosphorylated tau protein, a microtubule-associated protein. Since the cholinergic transmission is heavily impaired by the loss of

* Corresponding author. Tel.: +39 0805442782; fax: +39 0805442230.
E-mail addresses: angelo.carotti@uniba.it, carotti_angelo@hotmail.com (A. Carotti).

0223-5234/$ – see front matter © 2012 Elsevier Masson SAS. All rights reserved.
http://dx.doi.org/10.1016/j.ejmech.2012.10.003

cholinergic neurons in basal forebrain, current pharmacological therapies for AD rely chiefly on restoration of acetylcholine levels with acetylcholinesterase inhibitors (AChEIs) [6].

Aβ peptide, normally present as a soluble species in extracellular fluids, is mainly constituted by $A\beta_{1-40}$ and $A\beta_{1-42}$ (composed of 40 and 42 amino acids, respectively), originated from the enzymatic cleavage of amyloid precursor protein (APP) operated by secretases α and β. Aβ polymerizes through β-sheet ordered structures, in a multistep process involving the formation of several intermediate species, including soluble, low molecular weight oligomers and protofibrillar aggregates [7]. Several studies attribute the neurotoxicity and the progressive neurodegeneration of AD to these soluble intermediates rather than to mature amyloid fibrils or neuritic plaques [8]. Agents able to prevent or reverse fibrillization or, even better, the early oligomerization of Aβ may then have therapeutic potential in the treatment of AD [9].

Protein misfolding and aggregation are common hallmarks in many NDs [10]. As such, the inhibition of protein aggregation and related toxic events are under intense investigation, but to date, no valuable therapeutic agents have been discovered and all clinical trials with compounds acting on different targets have been unsuccessful [11].

Many chemical agents, either naturally occurring or produced by synthesis, and often containing planar (hetero)aromatic residues, can inhibit Aβ fibrillogenesis [12,13]. Antiamyloidogenic activity has been reported by some of us for glycine-based oligopeptides [14], indoles [15], isatins [16], tricyclic heteroaromatics [17] and anthraquinone drugs [18]. Recently, we also reported on a dynamic model of inhibition of Aβ aggregation [19], suggesting that specific π–π, hydrophobic and electrostatic/polar interactions, including hydrogen bonds, involving the backbone and some side chains of Aβ, led to the Aβ assembly. Disruption and/or prevention of these interactions by small molecules could trigger the inhibition of fibril formation.

Keeping in mind this array of interactions, as well as the ones taking place in the inhibition of cholinesterases, largely studied by some of us [20], benzo[*e*][1,2,4]triazin-7(1*H*)-ones **I** and [1,2,4]-triazino[5,6,1-*jk*]carbazol-6-ones **II** (Chart 1) were selected as attractive heterocycles to investigate Aβ fibrillization inhibition, since they share a quinone/quinonimine moiety and an extended planar azaheterocyclic system, that are important molecular determinants for establishing π–π, hydrophobic and electrostatic/polar interactions with the aggregating Aβ peptide. Indeed, in a recent study we demonstrated that interactions of a quinone moiety with the Aβ peptide backbone can efficiently hamper the Aβ self-assembly to β-sheet strands, thus blocking the Aβ aggregation process [19].

Scaffold **I** is amenable for molecular decoration because it undergoes facile regioselective nucleophilic addition and electrophilic substitution, at the C6 and C8 positions, respectively [21–23], thus allowing the attainment of a large molecular diversity. Furthermore, as oxidative and non-oxidative silver-mediated palladium catalyzed cyclizations at C8 gave the triazafluoranthenone **II** [22], which is structurally related to biologically active canthinone alkaloids [24,25], **II** was also chosen as the second planar and more rigid scaffold for comparison.

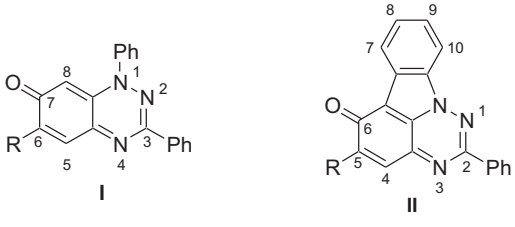

Chart 1. General structures of the examined benzotriazinones **I** and triazafluoranthenones **II**.

Benzotriazinones **3**–**28** (Table 1) and triazafluoranthenones **31**–**38** (Table 2) bearing mostly differently shaped amino substituents, were therefore prepared with the aim to i) discover potent Aβ aggregation inhibitors exhibiting an additional strong AChE and/or BChE inhibition to target AD, along the strategy of the multitargeted-ligands approach [26,27]; ii) delineate the structure–activity relationships (SARs) for further molecular optimization; and iii) improve physicochemical properties relevant for molecular bioactivity, including water solubility for easier and more reliable biochemical and pharmacological assays.

All compounds were assessed for their Aβ antiaggregating activity through the thioflavin T (ThT) spectrofluorimetric assay [28] and for their inhibitory activity toward AChE and BChE by the classical spectrophotometric test of Ellman [29].

Suitably selected compounds were subjected to a time course kinetic study by means of ThT fluorescence, CD signal at 215 nm and TEM micrographs to gain insights on the mechanism of inhibition and possibly on the targeted oligomeric species.

2. Chemistry

Readily available 1,3-diphenylbenzo[*e*][1,2,4]triazin-7(1*H*)-one **1** [30] and 2-phenyl-6*H*-[1,2,4]triazino[5,6,1-*jk*]carbazol-6-one **29** [22] were reacted with a series of nucleophiles to give the corresponding 6-substituted benzotriazinones **2**–**23**, **25**, **27** and **28** and 5-substituted triazafluoranthenones **30**–**37**, according to reported procedures [21,22] (Scheme 1).

Efforts to prepare the 6-({ϖ-[benzyl(methyl)amino]alkyl}(methyl)amino)-1,3-diphenylbenzo-[*e*][1,2,4]triazin-7(1*H*)-ones **24** (alkyl chain $n = 5$) or **26** (alkyl chain $n = 8$) by direct nucleophilic addition of N^1-benzyl-N^1,N^{ϖ}-dimethylalkane-1,ϖ-diamines to benzotriazinone **1** were unsuccessful owing to difficulties encountered in the preparation of the required diamine. Furthermore, although 6-[8-(*N*-benzyl-*N*-methylamino)octylamino]-1,3-diphenylbenzo[*e*][1,2,4]triazin-7(1*H*)-one **25** could be prepared directly from benzotriazinone **1** and the readily accessible *N*-methyl-*N*-benzyloctane-1,8-diamine [31], the subsequent N-methylation with either MeI or Me_2SO_4 suffered from overmethylation leading to the formation of quaternary salts. Therefore, the desired 6-({ϖ-[benzyl(methyl)amino]alkyl}(methyl)amino)-1,3-diphenylbenzo[*e*][1,2,4]triazin-7(1*H*)-ones **24** and **26** were prepared *via* a stepwise synthesis that involved preparing the 6-(methylamino)-1,3-diphenylbenzo[*e*][1,2,4]triazin-7(1*H*)-one **40**, its bromoalkyl derivatives 6-[(ϖ-bromoalkyl)(methyl)amino]-1,3-diphenylbenzo[*e*][1,2,4]triazin-7(1*H*)-ones **42** and **43** (alkyl chain $n = 5$ and 8, respectively) and their subsequent benzylmethylamination to give the desired products **24** and **26** (Scheme 2).

For the preparation of 5-{*N*-[8-(*N*-benzyl-*N*-methylamino)octyl]-*N*-methylamino}-2-phenyl-6*H*-[1,2,4]triazino[5,6,1-*jk*]carbazol-6-one (**38**) an additional difficulty was faced since the desired starting material 5-(methylamino)triazafluoranthenone could not be prepared directly because the treatment of triazafluoranthenone **29** with aqueous methylamine gave only very complex reaction mixtures. As the consequence, a strategy similar to that described above was adopted. Treatment of readily available 8-iodo-1,3-diphenylbenzo[*e*][1,2,4]triazin-7(1*H*)-one **39** [22], with aqueous methylamine gave 8-iodo-6-(methylamino)-1,3-diphenylbenzo[*e*][1,2,4]triazin-7(1*H*)-one **41** in 70% yield and subsequent reaction with 1,8-dibromooctane gave 6-[(8-bromooctyl)(methyl)amino]-8-iodo-1,3-diphenylbenzo[*e*][1,2,4]triazin-7(1*H*)-one **44** in 61% yield (Scheme 2). At this point attempted benzylmethylamination led mainly to protodeiodination. To avoid this undesirable side reaction

Table 1
Inhibition data of $A\beta_{1-40}$ aggregation, AChE and BChE of benzotriazinones **1**–**28**.

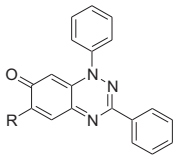

Entry	R	Aβ aggregation inhibition[a]	Cholinesterase inhibition[b]	
			AChE	BChE
1	H	(39)	(47)	(27)
2	CH_3O	(60)	(47)	(15)
3	$(C_2H_5)_2N$	17	(55)	(19)
4	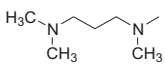	(45)	(46)	(18)
5		(68)	(54)	(15)
6		7.1	(39)	(7)
7		0.37	(0)	(22)
8	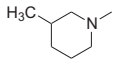	0.73	(55)	(25)
9	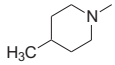	(68)	(48)	(11)
10	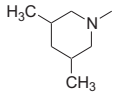	1.2	(46)	(18)
11	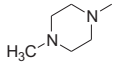	(55)	(55)	(12)
12		(48)	(42)	(0)
13		(62)	(42)	(0)
14	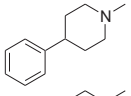	1.5	(35)	(10)
15	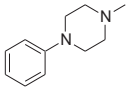	(53)	2.2	(15)
16	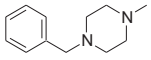	(61)	(56)	(18)
17		2.8	(46)	(47)
18		4.0	(55)	(37)
19		(13)	(57)	(9)
20		(51)	(57)	(11)

Table 1 (*continued*)

Entry	R	Aβ aggregation inhibition[a]	Cholinesterase inhibition[b]	
			AChE	BChE
21		(42)	(49)	(6)
22	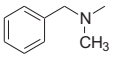	1.0	(56)	(22)
23	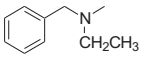	2.1	(53)	(13)
24	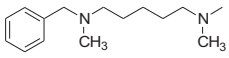	1.4	1.5	1.9
25	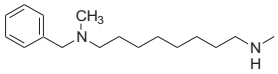	21	(45)	(28)
26	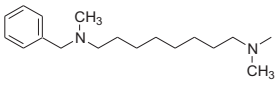	65	(50)	0.31
27		6.7	(41)	(10)
28	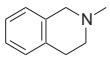	(68)	(47)	(14)

Data are means of three independent experiments; SEM < 10%.
[a] IC_{50} (μM) or inhibition % at 100 μM concentration (in parentheses).
[b] IC_{50} (μM) or inhibition % at 10 μM concentration (in parentheses).

the non oxidative Pd and AgF mediated cyclization [21], to give 5-[*N*-(8-bromooctyl)-*N*-methylamino]-2-phenyl-6*H*-[1,2,4]triazino[5,6,1-*jk*]carbazol-6-one **45** in moderate yield (39%), was carried out. The triazafluoranthenone **45** readily underwent benzylmethylamination to give the desired product **38** in 90% yield (Scheme 3).

3. Biological assays

In vitro inhibition of $A\beta_{1-40}$ aggregation was assessed following a previously reported ThT fluorescence-based method involving the use of hexafluoroisopropanol (HFIP) as aggregation enhancer [14–16]. Samples of Aβ were coincubated with test molecules at 100 μM in phosphate buffered saline (PBS) containing 2% HFIP and up to 10% v/v of DMSO as the cosolvents, and antiaggregating activities were measured after 2 h of incubation at 25 °C. For the most active compounds (≥80% Aβ aggregation inhibition) IC_{50} values were determined under the same assay conditions as already described [14–16]; data are reported in Tables 1 and 2. In order to confirm the antiaggregating activity of these new classes of compounds, inhibitors **7**, **24**, **29** and **38** were also tested for their activity on $A\beta_{1-42}$ aggregation (Fig. 4).

Inhibitory activities on AChE (from electric eel) and BChE (from equine serum) were determined by the spectrophotometric method of Ellman et al. [29] and are reported in Tables 1 and 2 as IC_{50} (μM) for the most active compounds, or as percentage of inhibition at 10 μM for compounds with low activity.

4. Transmission electron microscopy (TEM)

TEM analysis was performed at 39,000-fold magnification for samples of coincubated $A\beta_{1-40}$ (50 μM) with compounds **24**

Table 2
Inhibition data of $A\beta_{1-40}$ aggregation, AChE and BChE of triazafluoranthenones **29**–**38**.

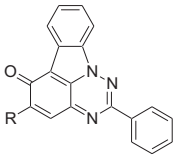

Entry	R	Aβ aggregation inhibition[a]	Cholinesterase inhibition[b]	
			AChE	BChE
29	H	6.1	(46)	(59)
30	CH_3O	(33)	(52)	(11)
31	$(C_2H_5)_2N$	1.4	(46)	(54)
32	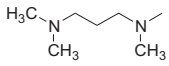	7.6	(49)	4.0
33		2.0	(44)	(52)
34	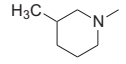	5.5	(27)	(53)
35	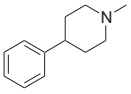	3.9	(48)	(11)
36	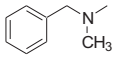	4.1	(53)	(26)
37	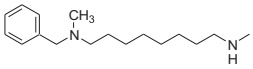	(60)	(46)	(25)
38	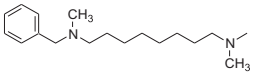	1.4	(55)	0.025

Data are means of three independent experiments; SEM < 10%.
[a] IC_{50} (μM) or inhibition % at 100 μM concentration (in parentheses).
[b] IC_{50} (μM) or inhibition % at 10 μM concentration (in parentheses).

(10 μM) and **29** (50 μM), compared with a free incubation sample of Aβ. Incubations were run using ethanol as the co-solvent (10% v/v) in PBS at the temperature of 37 °C, in order to achieve the complete Aβ aggregation within 10 days.

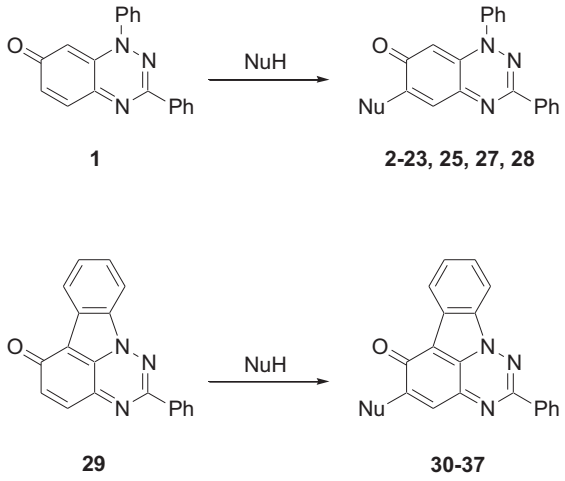

Scheme 1. Reagents and conditions: suitable amine or alcohol (NuH, excess), anhydrous THF, reflux.

5. CD spectroscopy

CD spectra were recorded in the spectral range 195–250 nm, following the conformational random coil to β-sheet transition as revealed by the increase of the negative peak of CD signal at 215 nm. Reference Aβ, and coincubated samples of Aβ/compound **24** and Aβ/compound **29** were prepared as above described for TEM studies.

6. Results and discussion

Inhibition data listed in Tables 1 and 2 were analyzed to derive structure–activity relationships and eventual insights in potential mechanism of action toward the different targets.

Some interesting considerations can be made by comparing biochemical data in Tables 1 and 2 for the two sets of products bearing the same substituent. With some notable exceptions, triazafluoranthenones (Table 2) were more active than the corresponding benzotriazinones (Table 1). This is evident for lead compounds (compare **29**, IC_{50} = 6.1 μM with **1**, 39% inhibition at 100 μM), **31** (1.4 μM) *vs.* **3** (17 μM), **32** (7.6 μM) *vs.* **4** (45%), **33** (2.0 μM) *vs.* **5** (68%), **38** (1.4 μM) *vs.* **26** (65 μM). In contrast, other couples of equally substituted inhibitors showed an inverted order of activity (compare **34** *vs.* **8**, **36** *vs.* **20** and **37** *vs.* **25**) or were nearly equipotent (**30** *vs.* **2**, **35** *vs.* **14**). Although restricted to fewer derivatives than benzotriazinones, triazafluoranthenones could be considered as a very active class of compounds showing, with only two exceptions (comps. **30** and **37**) an Aβ antiaggregating activity in the low micromolar range.

Within the set of benzotriazinones, compounds **7** and **8** emerged as highly potent inhibitors of Aβ fibrillization, with IC_{50} values of 0.37 and 0.73 μM, respectively, significantly better than the average IC_{50} values reported so far in the literature either for inhibitors of Aβ self-aggregation (direct inhibitors) or for inhibitors of Aβ aggregation derived from the blocking of the peripheral binding site of AChE that promotes/accelerates Aβ aggregation itself (indirect inhibitors) [32]. Within the class of benzotriazinones, piperidine derivatives **6**, **10** and **14** showed interesting activities with IC_{50} values of 7.1, 1.2 and 1.5 μM, respectively. Although benzotriazinones accounted for a high degree of substituent diversity, only some limited SAR could be derived. While small (**1**–**5**) and aromatic (**19**–**21**) substituents characterized low active compounds, the unsubstituted piperidine derivative **6** displayed an activity higher than the corresponding pyrrolidine derivative **5** (IC_{50} = 7.1 μM *vs.* 68% inhibition at 100 μM). Very surprisingly, while the 2- and 3-methylpiperidine derivatives **7** and **8** resulted the most active inhibitors, the 4-methyl regioisomer **9** exhibited a much lower inhibitory potency (68% inhibition), in contrast also to the 4-phenyl analog **14** that had high activity (IC_{50} 1.5 μM). Isosteric substitution in the piperidine ring was also detrimental as can be seen by comparing the poor activity of 1-morpholinyl and 1-thiomorpholinyl derivatives **12** and **13** (48 and 62% inhibition, respectively) with the piperidinyl one **6**. Piperazine derivatives showed a mixed and somehow unpredictable behavior: while comp. **11** retained the same low activity of the piperidine analog **9**, 4-phenylpiperazine derivative **15**, unlike its close 4-phenylpiperidine analog **14**, held the same low potency (53% inhibition), similar to its 4-*N*-benzyl homologue **16** (61%).

The introduction of larger cyclic (comp. **17**) or bicyclic amines (comps. **27** and **28**) had the same controversial effect. While 1-azepinyl and 1-quinolinyl derivatives **17** and **27** were good inhibitors of Aβ fibrillization (IC_{50} = 2.8 μM and 6.7 μM, respectively), 2-isoquinolinyl analog **28** again suffered a strong drop of activity (68% inhibition). In this case, when comparing the activity of **28** with open-chain analogs **22** (IC_{50} = 1.0 μM) and **23** (2.1 μM), a detrimental effect due to a molecular rigidification could be

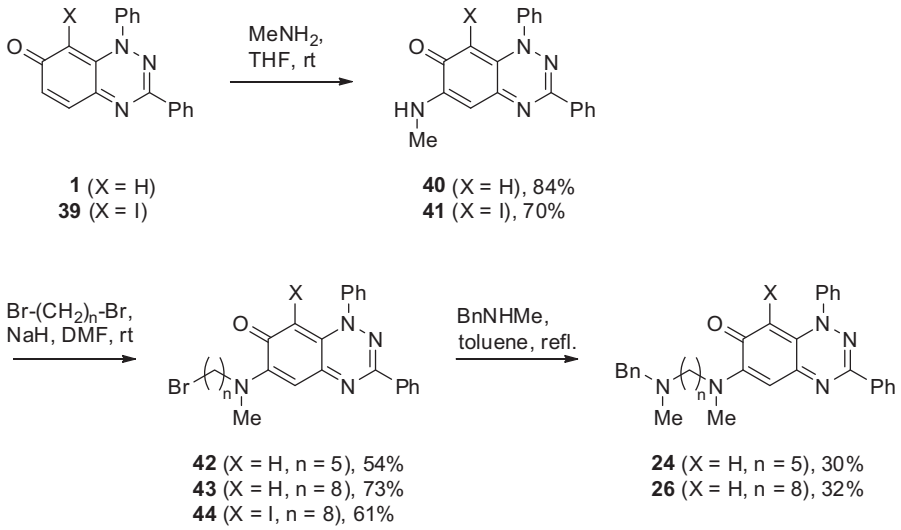

Scheme 2. Synthesis of compounds **24** and **26**.

claimed. Finally, it is worth noting that *N*-alkyl-*N*-benzyl derivatives **22** and **23** were significantly more active than the corresponding anilino derivative **20**, and that the substitution of phenyl ring of **20** with a cyclohexyl in comp. **18** led to a potent inhibitor ($IC_{50} = 4.0$ μM) of Aβ aggregation.

Compounds **22**–**26**, **37** and **38** were designed and prepared with the aim to fully address, besides Aβ aggregation process, the inhibition of AChE and/or BChE. They all bore the *N*-methyl-*N*-benzylamino moiety as a typical structural determinant for cholinesterase inhibition, due to a likely binding at the catalytic site, either connected directly to the benzotriazinone scaffold (**22** and **23**) or spaced by linear alkyl chains of different length (**24**–**26**, **37** and **38**). Compounds **22** and **23** and the pentamethylene-bridged compound **24**, all showed a very potent activity against Aβ aggregation (IC_{50} values in the range 1–2 μM). Interestingly, compound **24** was very active also as AChE and BChE dual inhibitor showing IC_{50} values of 1.5 and 1.9 μM, respectively. The very well balanced and strong inhibitory activities of **24** make this compound a promising candidate for further in vitro and in vivo studies in AD animal models.

The elongation of the bridging linker to an octamethylene resulted in the lowering of both antiaggregating and cholinesterase activities, with the notable exception of comp. **26** and its fused analog **38**, which exhibited a very potent and selective inhibition of BChE ($IC_{50} = 0.31$ and 0.025 μM, respectively). The inhibitory potency of **38** was outstanding compared with the average literature data on selective BChE inhibitors [33]. Very surprisingly, its *N*-demethylated analog **37** lacked both anti-Aβ and cholinesterase activity. A similar behavior was observed for the benzotriazinones **25** and **26**: The *N*-Me derivative **26** displayed a BChE inhibition much stronger than the corresponding NH analog **25** and this may suggest some critical and selective interactions of the 6-NMe group of **26** and **38** into the BChE binding site.

The attractiveness of some of the most active benzotriazinones and triazafluoranthenones as potential hit molecules for an in vivo screening on animal models of AD [34] and for the evaluation of additional biopharmacological activities may be limited by their poor bioavailability and aqueous solubility.

Taking into account that the ThT test does not provide any evidence about the actual mechanism of inhibition, being only indicative of the presence of fibrillar aggregates, and that false positives might emerge [35], a battery of parallel ThT/CD/TEM experiments was designed and performed to assess the effects of selected inhibitors over the temporal evolution of $A\beta_{1-40}$

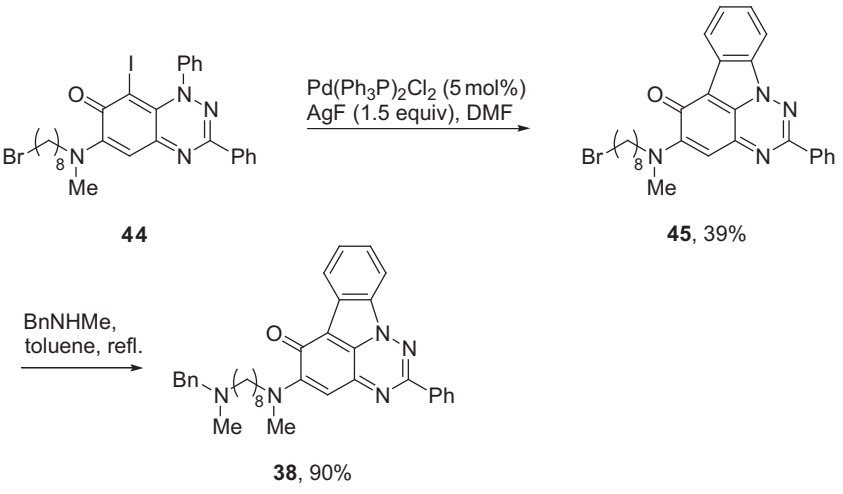

Scheme 3. Synthesis of compound **38**.

fibrillization. Besides ThT fluorescence, circular dichroism (CD) spectroscopy, which accounts for conformational changes of the monomeric random coil $A\beta_{1-40}$ to β-sheet ordered amyloidogenic intermediates, was used [36]. The characterization of quantity, shape and dimension of aggregates formed was finally investigated with transmission electron microscopy (TEM). Since coincubation had to be made in aqueous buffer (PBS) and only a limited aliquot (10%) of the ethanol as cosolvent can be allowed, the selection of molecules to be tested was made after an accurate preliminary measure of their solubility in the assay medium, by means of UV spectroscopy (data not shown). From this solubility screening benzotriazinone **24** and triazafluoranthenone **29** emerged as the most promising compounds in terms of aqueous solubility and Aβ antiaggregating activity; they were therefore chosen and tested at their allowed maximum solubility in the incubation assay medium (10 and 50 μM, respectively).

Stock solutions of **24** and **29** were prepared in ethanol, avoiding the use of DMSO which is non-transparent for CD measures. Free aggregation samples, containing $A\beta_{1-40}$ (50 μM) alone or with test inhibitors, were incubated at 37 °C without agitation. Aliquots were removed at various time points and analyzed by ThT fluorescence and CD spectroscopy (Figs. 1 and 2). The fibrillization evolved with a typical sigmoidal increase of fluorescence, accounting for a nucleation-dependent process, with an initial lag phase of three days and an exponential growth going to completion between days 3 and 6. Both **24** and **29** acted as strong inhibitors of the fibrillization process that lacked the exponential growth phase and reached only 30–40% of fluorescence of the control peptide (full lines in Fig. 1). Evolution of the CD spectra showed for the free incubation control sample the same sigmoidal shape with attainment of plateau at day 6. The random coil to β-sheet transition was measured as the absolute value of the typical negative peak of ellipticity at 215 nm (dotted lines in Fig. 1). CD data of the coincubated samples were contrasting and highlighted an inhibitory behavior quite different for the two examined inhibitors. While **24** acted on β-sheet transition in a parallel way to fibrillization process, delaying the exponential phase and lowering the β-sheet content to 40% of control peptide, the co-incubated sample of **29** showed a dramatic increment between days 3 and 4, reaching and stabilizing a β-sheet configuration even at a greater extent than reference Aβ alone (Fig. 2). This feature can be rationalized hypothesizing for compound **29** a strong stabilization of its complex with β-sheet arranged peptide, hampering the further aggregation to mature fibrils, while compound **24** appeared instead to act as stabilizer of random coil arranged, unstructured peptide.

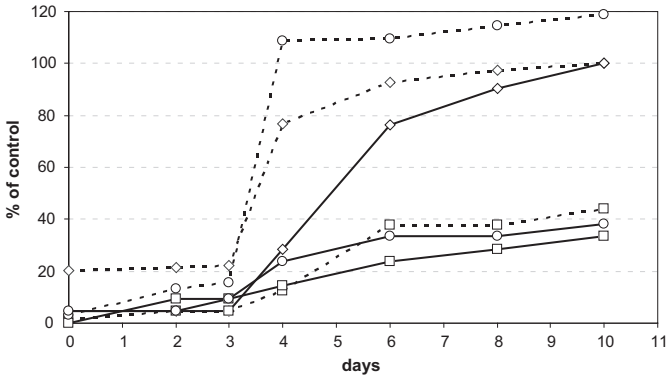

Fig. 1. Time-course aggregation kinetics of $A\beta_{1-40}$ control (diamonds), Aβ/**24** (squares) and Aβ/**29** (circles). Results are expressed as percentage of the final value of ThT fluorescence (full lines) and CD ellipticity at 215 nm (dotted lines), both attained at the plateau of the fibrillization reaction of control peptide.

TEM micrographs (Fig. 3) highlighted the fibrillization of $A\beta_{1-40}$ control peptide that gave rise after 7 days to an extensive formation of thin and long fibrils (Fig. 3B). While the effects of compound **24** were consistent with ThT and CD measures, leading only to isolated fibrillar aggregates (Fig. 3C), samples co-incubated with compound **29** showed an extended fibrillar weft (Fig. 3D). Since ThT results clearly stated for both coincubation samples Aβ/**24** and Aβ/**29** a very similar and significant decrease of fluorescence compared with reference Aβ (Fig. 1), it must be deduced that filaments in Fig. 3D could be protofibrillar species that are clearly detected by CD, although being transparent to ThT fluorescence measures. Resolution of TEM micrographs, however, did not allow a precise evaluation of diameter and shape of such aggregates, which appear as quite similar to fibrils formed in free Aβ aggregation. Once again, the TEM results for triazafluoranthenone **29** are controversial and need further biophysical evaluation to assess the mechanism of $A\beta_{1-40}$ aggregation inhibition and the actual intermediate species formed/targeted. Unfortunately, the poor water solubility of our compounds precluded the use of capillary electrophoresis (CE) to clarify such an issue. CE indeed has been an efficient separation and detection technique largely used by us to identify in a non-ambiguous manner the oligomeric species of Aβ targeted by inhibitors of different classes of compounds [18].

Amyloid peptide $A\beta_{1-42}$ represents the predominant form in AD brain, respect to $A\beta_{1-40}$, and it is also more toxic and prone to aggregation. It is also well known that $A\beta_{1-42}$ quickly aggregates in common in vitro tests, leading to fibril formation in shorter time than $A\beta_{1-40}$. Although $A\beta_{1-40}$ is more handable and commercially cheaper, and for these reasons is often preferred for in vitro tests, the measure of antiaggregating effect even on $A\beta_{1-42}$ should give a more complete information on the inhibitory behavior of any new class of substances. For these reasons we did also perform a suitable inhibition test of $A\beta_{1-42}$ aggregation for few selected compounds, by measuring the ThT fluorescence of a coincubation sample of 100 μM inhibitor with 30 μM $A\beta_{1-42}$ in PBS/10% DMSO at 37 °C [37]. Along with the most active inhibitor **7**, we tested compounds **24** and **29** already selected for time course kinetic experiments, and finally **38** as the most interesting dual Aβ/BChE inhibitor. As reference compound to validate the reliability of our results, we used quercetin, a well established inhibitor of amyloid aggregation [14]. Very satisfactorily, experimental results (Fig. 4) were in full agreement with those determined for $A\beta_{1-40}$. In particular, ThT fluorescence of coincubation samples was always quite lower than self aggregating peptide used as control (Fig. 4) at both 8 h and 24 h time points, thus confirming the Aβ antiggregating activity of these two classes of substances.

7. Conclusions

Benzotriazinones **1**–**28** and triazafluoranthenones **29**–**38** were designed and prepared to address two major therapeutic targets involved in AD, beta-amyloid self-aggregation and cholinesterase activity. The presence of a quinonimine motif in both planar aza-heterocyclic scaffolds suggested a possible activity either as β-sheet disrupting or β-sheet formation preventing agents, while their easy synthetic decoration allowed the introduction of different substituents, in particular protonatable amines able to interact with the catalytic site of cholinesterases. The underlying goal was to provide new chemical entities able to act as dual active agents, within the so-called multitarget approach to handle different pathological features of AD and possibly other multifactorial NDs.

From the ThT-based fluorimetric test, a number of compounds were identified as potent inhibitors of $A\beta_{1-40}$ aggregation, with IC_{50} values spanning from 0.37 to 65 μM. 6-(2-Methylpiperidin-1-yl)-benzotriazinone **7** emerged as the most potent inhibitor (IC_{50}

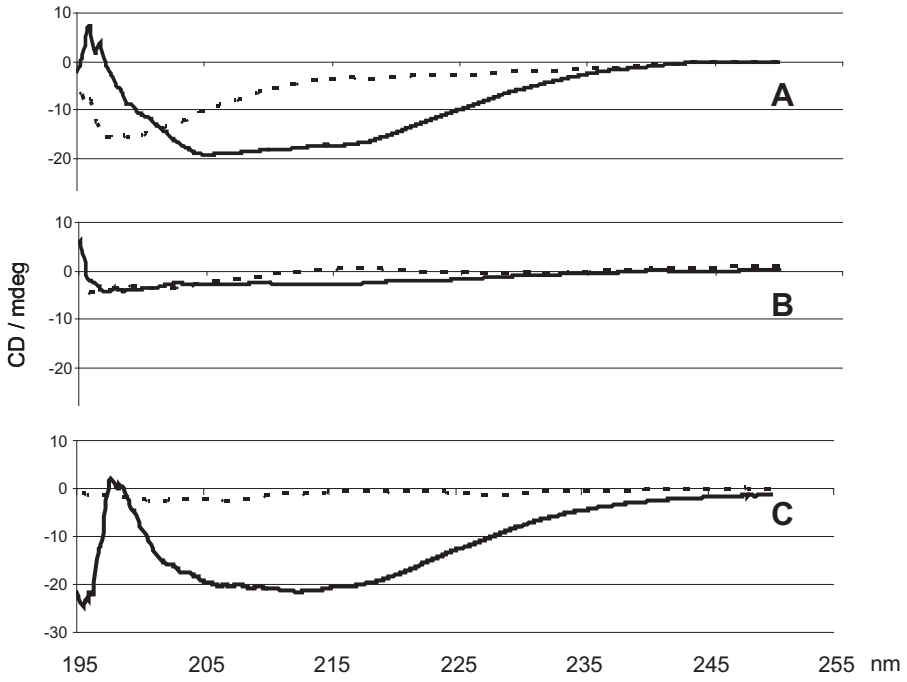

Fig. 2. Circular dichroism spectra of aggregating $A\beta_{1-40}$ alone (A) and coincubated with inhibitors **24** (B) and **29** (C) in PBS/10% ethanol at 37 °C. Dotted lines: CD spectrum at time point zero; full lines: CD spectra after 7 days.

0.37 μM), while several other compounds from both series exhibited low to submicromolar IC_{50} values. With some notable exceptions, triazafluoranthenones were more active than the corresponding benzotriazinones bearing the same substituents, suggesting a favorable role of a more extended planarity and rigidity in hydrophobic interactions with aggregation-prone Aβ peptide sequence.

Anticholinergic activity was measured on both AChE and BChE through the classical Ellman's test. Two closely related compounds **26** and **38**, bearing the heterocyclic scaffolds tethered to an N(Me)Bn moiety through an octamethylene linker, showed a very potent and selective inhibition of BChE. In particular triazafluoranthenone **38** had an impressive IC_{50} (25 nM) and a high BChE over AChE selectivity. Only a few other compounds, all bearing a basic moiety as substituent, gave good and somewhat selective inhibition of AChE (**15**), BChE (**32**) or acted as dual inhibitors (**24**).

To gain insights on the inhibitory mechanism of Aβ aggregation, benzotriazinone **24** and triazafluoranthenone **29** were selected for a time course kinetic study by means of ThT fluorescence, CD signal at 215 nm and TEM micrographs. Experimental data suggested that **24** might act as β-sheet disrupter while **29** might enhance and stabilize the β-sheet arrangement of Aβ. In both cases the ultimate effect was the inhibition of fibrillization, as detected by ThT and confirmed, at least for **24**, by TEM.

The antiaggregating behavior of these two classes of compounds was finally confirmed also on $A\beta_{1-42}$ peptide, by means of a coincubation test that allowed to assess that compounds **7**, **24**, **29** and **38** also acted as strong inhibitors of $A\beta_{1-42}$ fibrillogenesis.

Since prefibrillar oligomers of Aβ, and not mature fibrils, are responsible for neuronal damage in AD [8], it could be claimed that compound **24** and some of its close analogs may deserve further investigations, aimed at discovering the nature and toxicity of the oligomeric intermediates targeted by **24**. The good inhibitory activity of **24** on both cholinesterases represents another qualifying feature of this compound.

The high BChE inhibitory activity of triazafluoranthenone **38** also emerged as an outstanding result, even considering its very good antiaggregating activity, although the exact role of BChE and its selective inhibition in AD is still debated [33].

The poor aqueous solubility and the potential low bioavailability would be important drawbacks of the two classes of compounds examined herein, only partially overcome by their high potencies. In this perspective, the evaluation of derivatives bearing more hydrophilic substituents will be a mandatory evolution of the study reported herein along with an assessment (and optimization) of ADMET properties. Eventually, pharmacological data from animal models of AD are needed to confirm the validity of the multi-targeted ligands approach in AD.

8. Experimental

8.1. General methods and materials

All commercial chemicals and reagents were purchased from Sigma–Aldrich and used without further purification unless otherwise specified. DCM was freshly distilled from CaH_2 under argon. Reactions were protected from atmospheric moisture by $CaCl_2$ drying tubes. Anhydrous Na_2SO_4 was used for drying organic extracts, and all volatiles were removed under reduced pressure. All reaction mixtures and column eluents were monitored by TLC using commercial glass backed thin layer chromatography (TLC) plates (Merck Kieselgel 60 F_{254}). The plates were observed under UV light at 254 and 365 nm. The technique of dry flash chromatography was used throughout for all non-TLC scale chromatographic separations using Merck Silica Gel 60 (less than 0.063 mm). Melting and decomposition points were determined using either a PolyTherm-A, Wagner & Munz, Koefler-Hotstage Microscope apparatus or a TA Instruments DSC Q1000 with samples hermetically sealed in aluminum pans under an argon atmosphere, using

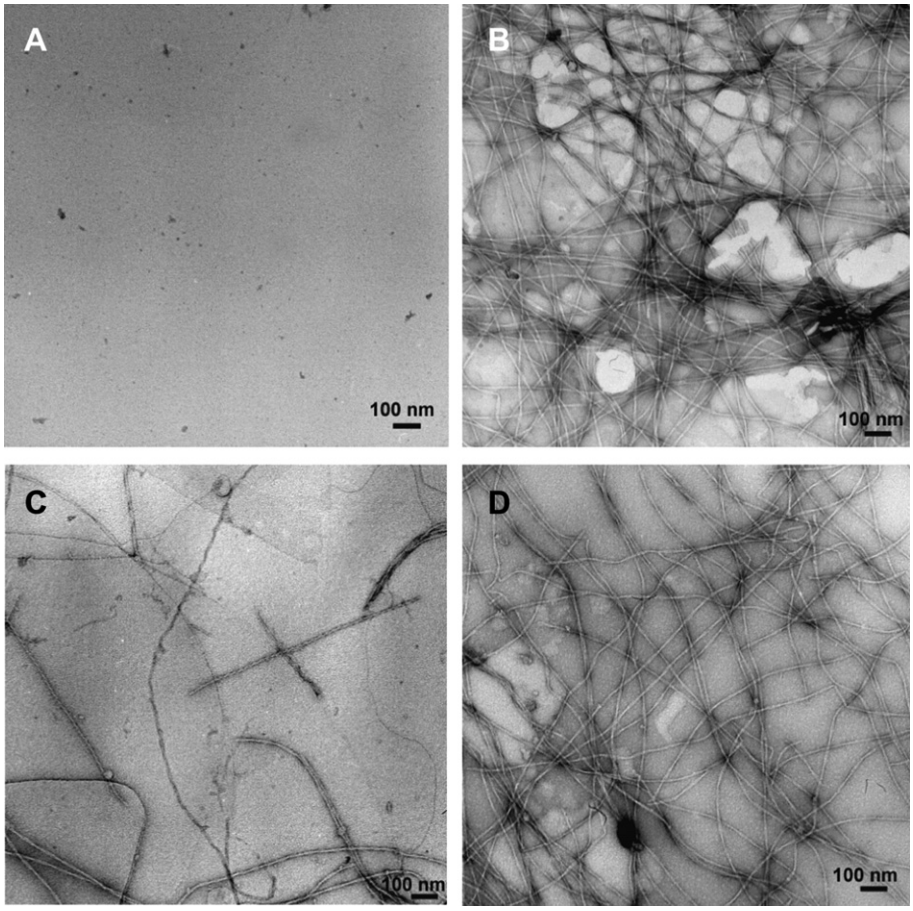

Fig. 3. Effects of inhibitors **24** and **29** on $A\beta_{1-40}$ aggregation. $A\beta_{1-40}$ (50 μM) was incubated under fibrillization conditions alone or in the presence of 10 μM **24** or 50 μM **29**. Aliquots of each reaction were assayed by TEM (39 000-fold magnification): for control reaction at time point zero (A) and after 7 days (B); for coincubated Aβ/**24** (C) and Aβ/**29** (D) after 7 days.

heating rates of 5 °C/min. Solvents used for recrystallization are indicated after the melting point. UV spectra were obtained using a Perkin–Elmer Lambda-25 UV/vis spectrophotometer and inflections are identified by the abbreviation 'inf'. IR spectra were recorded on a Shimadzu FTIR-NIR Prestige-21 spectrometer with a Pike Miracle Ge ATR accessory and strong, medium and weak peaks are represented by s, m and w, respectively. ^1H and ^{13}C NMR spectra were recorded on a Bruker Avance 300 machine (at 300 and 75 MHz, respectively) and on a Bruker Avance 500 machine (at 500 and 125 MHz, respectively). Deuterated solvents were used for homonuclear lock and the signals are referenced to the deuterated solvent peaks. Low resolution (EI) mass spectra were recorded on a Shimadzu Q2010 GC/MS with direct inlet probe.

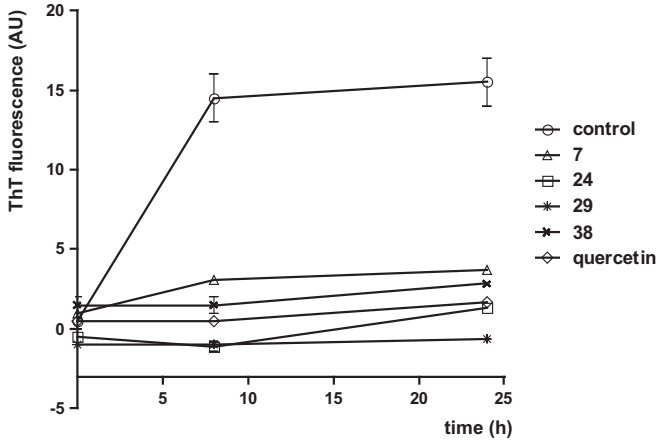

Fig. 4. ThT fluorescence assay for the inhibition of $A\beta_{1-42}$ aggregation of compounds **7**, **24**, **29** and **38**. Points are ThT fluorescence values (arbitrary units) registered at various time points for 30 μM peptide alone (control) and coincubated with 100 μM test compounds. Quercetin was used as reference compound [14,37]. Data are means of three independent experiments ± SEM.

Benzotriazinones **1** [30], **2** [22], **3** [22], **5** [22], **6** [21], **11** [21], **15** [21], **18**–**21** [21], **28** [21], **39** [22], triazafluoranthenones **29**–**31** [22], **33** [22] and *N*-methyl-*N*-benzyloctane-1,8-diamine [31] were prepared according to the literature methods.

*8.2. Preparation of 6-substituted benzotriazinones **4**, **7**–**10**, **12**–**14**, **16**, **17**, **22**, **23**, **25**, **27***

A stirred mixture of 1,3-diphenylbenzo[*e*][1,2,4]triazin-7(1*H*)-one (**1**) (100 mg, 0.334 mmol) and alkylamine (7.5 mmol) in THF (1 mL) was heated at *ca.* 80 °C for 1 h. The reaction mixture was allowed to cool to rt, diluted with DCM (20 mL) and washed with 10% HCl (2 × 10 mL). The organic layer was separated, dried (Na_2SO_4), filtered, adsorbed onto silica and chromatographed to give the desired product.

*8.2.1. 6-{N-[3-(Dimethylamino)propyl]-N-methylamino}-1,3-diphenylbenzo[e][1,2,4]-triazin-7(1H)-one (**4**)*

Orange needles (98%). Mp: 233–234°C (from EtOH), R_f (DCM/MeOH, 1:5) 0.39; λ_{max}(DCM)/nm 278 (log ε, 3.22), 298 (3.29), 318 inf (3.17), 342 inf (2.80), 358 inf (2.72), 431 inf (3.10), 449 (3.20);

ν_{max}/cm^{-1} 1587 m, 1535 s, 1510 m, 1481 m, 1450 m, 1393 m, 1360 m, 1315 m, 1298 m, 814 m, 775 m; δ_H (300 MHz, $CDCl_3$) 8.30–8.27 (2H, m, Ar *H*), 7.62–7.54 (5H, m, Ar *H*), 7.48–7.45 (3H, m, Ar *H*), 6.75 (1H, s, Ar *H*), 6.00 (1H, s, Ar *H*), 4.09 (2H, t, *J* 6.9, CH_2), 3.21 (3H, s, CH_3), 3.20–3.12 (2H, m, CH_2), 2.82 (6H, s, 2CH_3), 2.45–2.32 (2H, m, CH_2); δ_C (75 MHz, $CDCl_3$) 1 × Ar CH peak missing, 176.5 (s), 154.6 (s), 152.7 (s), 152.4 (s), 141.6 (s), 135.2 (s), 135.0 (s), 130.1 (d), 129.8 (d), 128.6 (d), 126.9 (d), 125.9 (d), 103.2 (d), 97.2 (d), 55.7 (t), 50.6 (t), 43.1 (q), 40.4 (q), 24.5 (t); *m*/*z* (EI) 413 (M^+, 4%), 355 (2), 342 (36), 327 (15), 313 (15), 285 (2), 180 (3), 168 (2), 84 (5), 77 (11), 58 (100). Anal calcd for $C_{25}H_{27}N_5O$ (413.51): C 72.61, H 6.58, N 16.94. Found: C 72.56, H 6.49, N 17.03.

8.2.2. 6-(2-Methylpiperidin-1-yl)-1,3-diphenylbenzo[e][1,2,4]triazin-7(1H)-one (**7**)

Orange needles (49%). Mp: 158–159 °C (EtOH aq.), R_f (Et_2O) 0.56; λ_{max}(DCM)/nm 281 inf (log ε 3.63), 302 (3.84), 349 inf (3.18), 365 inf (3.01), 442 (3.51), 458 (3.55); ν_{max}/cm^{-1} 1584 m, 1530 s, 1493 m, 1449 m, 1315 m, 1306 m, 1258 m, 1180 m, 1140 m, 1126 m, 891 m, 835 m, 820 m, 781 m, 773 m; δ_H (300 MHz, $CDCl_3$) 8.29–8.24 (2H, m, Ar *H*), 7.59–7.53 (5H, m, Ar *H*), 7.49–7.42 (3H, m, Ar *H*), 6.85 (1H, s, Ar *H*), 6.05 (1H, s, Ar *H*), 4.97 (1H, br s, C*H*N), 4.44 (1H, br d, *J* 11.7, C*H*N), 3.29–3.19 (1H, m, C*H*Me), 1.97–1.44 (6H, m, CH_2), 1.37–1.32 (3H, d, *J* 6.6, CH_3); δ_C (75 MHz, $CDCl_3$) 177.5 (s), 156.5 (s), 152.9 (s), 151.8 (s), 141.8 (s), 135.6 (s), 134.7 (s), 129.8 (d), 129.7 (d), 129.6 (d), 128.5 (d), 126.8 (d), 125.9 (d), 104.8 (d), 97.6 (d), 51.5 (d), 43.45 (t), 30.8 (t), 25.9 (t), 18.7 (t), 15.6 (q); *m*/*z* (EI) 396 (M^+, 100%), 381 (10), 353 (8), 339 (14), 327 (10), 314 (27), 299 (11), 271 (6), 198 (9), 168 (7), 144 (5), 118 (6), 104 (8), 91 (11), 77 (46), 63 (5), 55 (10), 51 (10). Anal calcd for $C_{25}H_{24}N_4O$ (396.48): C 75.73, H 6.10, N 14.13. Found: C 75.78, H 6.12, N 14.04.

8.2.3. 6-(3-Methylpiperidin-1-yl)-1,3-diphenylbenzo[e][1,2,4]triazin-7(1H)-one (**8**)

Orange needles (86%). Mp: 170–171°C (from cyclohexane), R_f (Et_2O) 0.53; λ_{max}(DCM)/nm 280 inf (log ε 3.35), 303 (3.41), 321 inf (3.29), 347 inf (2.90), 361 inf (2.78), 459 (3.33); ν_{max}/cm^{-1} 1591 m, 1535 s, 1495 m, 1449 m, 1315 m, 1294 m, 1285 m, 1236 m, 1204 m, 968 m, 901 m, 845 m, 824 m, 779 m, 745 m; δ_H (300 MHz, $CDCl_3$) 8.28–8.25 (2H, m, Ar *H*), 7.58–7.52 (5H, m, Ar *H*), 7.49–7.42 (3H, m, Ar *H*), 6.85 (1H, s, Ar *H*), 6.06 (1H, s, Ar *H*), 4.63 (1H, d, *J* 11.7, CH_2), 4.48 (1H, d, *J* 12.3, CH_2), 3.09 (1H, ddd, *J* 12.3, 12.3, 3.2, CH_2), 2.82 (1H, dd, *J* 12.9, 10.8, CH_2), 1.91–1.65 (4H, m, CH_2), 1.31–1.19 (1H, m, C*H*), 0.98–0.95 (3H, d, *J* 6.3, CH_3); δ_C (75 MHz, $CDCl_3$) 177.2 (s), 155.7 (s), 152.7 (s), 151.8 (s), 141.7 (s), 135.4 (s), 134.7 (s), 129.8 (d), 129.7 (d), 129.6 (d), 128.5 (d), 126.75 (d), 125.9 (d), 104.5 (d), 97.5 (d), 56.8 (t), 50.0 (t), 33.2 (t), 31.7 (d), 25.6 (t), 19.1 (q); *m*/*z* (EI) 396 (M^+, 100%), 381 (8), 353 (6), 341 (14), 314 (19), 299 (13), 271 (8), 198 (6), 168 (9), 116 (5), 104 (6), 84 (5), 77 (37), 55 (8), 51 (7). Anal calcd for $C_{25}H_{24}N_4O$ (396.48): C 75.73, H 6.10, N 14.13. Found: C 75.83, H 6.24, N 14.28.

8.2.4. 6-(4-Methylpiperidin-1-yl)-1,3-diphenylbenzo[e][1,2,4]triazin-7(1H)-one (**9**)

Orange needles (99%). Mp: 170–171 °C (EtOH aq.), R_f (Et_2O) 0.51; λ_{max}(DCM)/nm 280 inf (log ε 3.34), 303 (3.40), 322 inf (3.28), 347 inf (2.89), 362 inf (2.74), 458 (3.33); ν_{max}/cm^{-1} 1585 m, 1530 s, 1485 m, 1447 m, 1315 m, 1233 m, 1200 m, 1076 m, 829 m, 820 m, 775 m, 746 m; δ_H (300 MHz, $CDCl_3$) 8.27–8.24 (2H, m, Ar *H*), 7.57–7.49 (5H, m, Ar *H*), 7.44–7.42 (3H, m, Ar *H*), 6.85 (1H, s, Ar *H*), 6.05 (1H, s, Ar *H*), 4.63 (2H, d, *J* 12.3, CH_2), 3.09 (2H, t, *J* 12.3, CH_2), 1.99 (1H, br s, C*H*), 1.80–1.70 (2H, m, CH_2), 1.45–1.33 (2H, m, CH_2), 0.97 (3H, d, *J* 6.3, CH_2); δ_C (75 MHz, $CDCl_3$) 177.2 (s), 155.8 (s), 152.7 (s), 151.7 (s), 141.7 (s), 135.4 (s), 134.7 (s), 129.8 (d), 129.6 (d), 129.5 (d), 128.4 (d), 126.7 (d), 125.8 (d), 104.7 (d), 97.5 (d), 49.7 (t), 34.3 (t), 31.0 (d), 21.6 (q); *m*/*z* (EI) 396 (M^+, 100%), 353 (7), 341 (5), 339 (7), 327 (9), 314 (12), 299 (15), 271 (8), 198 (5), 168 (7), 118 (4), 77 (28), 51 (7). Anal calcd for $C_{25}H_{24}N_4O$ (396.48): C 75.73, H 6.10, N 14.13. Found: C 75.85, H 6.09, N 14.13.

8.2.5. 6-(3,5-Dimethylpiperidin-1-yl)-1,3-diphenylbenzo[e][1,2,4]triazin-7(1H)-one (**10**)

Orange prisms (60%). Mp: 172–175 °C (from cyclohexane), R_f (THF/hexane, 1:1) 0.54; λ_{max}(DCM)/nm 281 (log ε 3.52), 304 (3.58), 322 inf (3.46), 346 inf (3.08), 439 inf (3.44), 460 (3.52); ν_{max}/cm^{-1} 1593 m, 1535 s, 1503 m, 1493 m, 1450 m, 1315 m, 1285 m, 1238 m, 1217 m, 1171 m, 1099 m, 905 m, 849 m, 824 m, 779 m; δ_H (300 MHz, acetone-d_6) 8.35–8.22 (2H, m, Ar *H*), 7.79–7.59 (5H, m, Ar *H*), 7.55–7.40 (3H, m, Ar *H*), 6.84 (1H, s, Ar *H*), 5.75 (1H, s, Ar *H*), 4.73 (2H, d, *J* 11.1, CH_2), 2.58 (2H, t, *J* 12.1, CH_2), 1.95–1.72 (3H, m, C*H*, CH_2), 1.05–0.83 (7H, m, C*H*, CH_2); δ_C (75 MHz, acetone-d_6) 1 × Ar CH peak missing, 177.3 (s), 156.0 (s), 153.9 (s), 151.7 (s), 143.0 (s), 136.6 (s), 135.5 (s), 130.7 (d), 130.5 (d), 129.3 (d), 127.3 (d), 127.0 (d), 104.9 (d), 97.6 (d), 56.7 (t), 43.1 (t), 32.5 (d), 19.3 (q); *m*/*z* (EI) 410 (M^+, 100%), 395 (12), 355 (22), 339 (5), 327 (14), 314 (23), 299 (11), 271 (5), 205 (6), 168 (6), 77 (21), 55 (6). Anal calcd for $C_{26}H_{26}N_4O$ (410.51): C 76.07, H 6.38, N 13.65. Found: C 76.22, H 6.23, N 13.53.

8.2.6. 6-Morpholino-1,3-diphenylbenzo[e][1,2,4]triazin-7(1H)-one (**12**)

Orange needles (93%). Mp: 204–206°C (from EtOH/cyclohexane), R_f (Et_2O) 0.24; λ_{max}(DCM)/nm 279 (log ε 3.40), 300 (3.41), 319 inf (3.36), 339 inf (3.10), 360 inf (2.93), 451 (3.32); ν_{max}/cm^{-1} 1597 m, 1589 m, 1547 s, 1510 m, 1491 m, 1456 m, 1315 m, 1285 m, 1240 m, 1200 m, 1121 s, 1097 m, 934 m, 901 s, 837 m, 820 m, 768 m, 718 m; δ_H (300 MHz, $CDCl_3$) 8.29–8.23 (2H, m, Ar *H*), 7.65–7.50 (5H, m, Ar *H*), 7.50–7.41 (3H, m, Ar *H*), 6.84 (1H, s, Ar *H*), 6.10 (1H, s, Ar *H*), 3.87 (8H, br s, CH_2); δ_C (75 MHz, $CDCl_3$) 176.7 (s), 155.7 (s), 152.9 (s), 151.7 (s), 141.4 (s), 134.9 (s), 134.6 (s), 130.0 (d), 129.8 (d), 129.75 (d), 128.5 (d), 126.7 (d), 125.8 (d), 105.6 (d), 97.6 (d), 66.6 (t), 49.0 (t); *m*/*z* (EI) 384 (M^+, 100%), 367 (5), 353 (6), 341 (87), 327 (52), 313 (16), 299 (17), 271 (9), 192 (7), 180 (8), 168 (12), 140 (7), 118 (10), 103 (12), 91 (8), 77 (53), 63 (9), 51 (14). Anal calcd for $C_{23}H_{20}N_4O_2$ (384.43): C 71.86, H 5.24, N 14.57. Found: C 71.92, H 5.22, N 14.75.

8.2.7. 6-Thiomorpholino-1,3-diphenylbenzo[e][1,2,4]triazin-7(1H)-one (**13**)

Purple needles (51%). Mp: 246–247°C (from EtOH/cyclohexane), R_f (Et_2O) 0.56; λ_{max}(DCM)/nm 281 (log ε 3.64), 292 (3.64), 320 inf (3.46), 347 inf (3.14), 362 inf (2.98), 431 inf (3.36), 433 (3.45); ν_{max}/cm^{-1} 1584 m, 1530 s, 1504 m, 1493 m, 1450 m, 1315 m, 1294 m, 1219 m, 1182 m, 961 m, 878 m, 826 m, 777 m; δ_H (300 MHz, $CDCl_3$) 8.29–8.26 (2H, m, Ar *H*), 7.60–7.55 (5H, m, Ar *H*), 7.48–7.45 (3H, m, Ar *H*), 6.90 (1H, s, Ar *H*), 6.12 (1H, s, Ar *H*), 4.25–4.22 (4H, m, CH_2), 2.86–2.82 (4H, m, CH_2); δ_C (75 MHz, $CDCl_3$) 176.7 (s), 155.2 (s), 152.8 (s), 151.9 (s), 141.5 (s), 135.0 (s), 134.7 (s), 130.1 (d), 129.9 (d), 129.8 (d), 128.6 (d), 126.8 (d), 125.8 (d), 105.6 (d), 97.8 (d), 52.0 (t), 27.5 (t); *m*/*z* (EI) 400 (M^+, 100%), 383 (6), 367 (56), 341 (42), 327 (33), 314 (10), 299 (16), 271 (6), 200 (5), 186 (6), 168 (9), 144 (6), 116 (7), 104 (9), 91 (6), 77 (61), 51 (13). Anal calcd for $C_{23}H_{20}N_4OS$ (400.50): C 68.98, H 5.03, N 13.99. Found: C 69.02, H 5.17, N 14.09.

8.2.8. 6-(4-Phenylpiperidin-1-yl)-1,3-diphenylbenzo[e][1,2,4]triazin-7(1H)-one (**14**)

Orange needles (93%). Mp: 200–201°C (from cyclohexane), R_f (Et_2O) 0.51; λ_{max}(DCM)/nm 281 (log ε 3.47), 302 (3.53), 321 inf (3.42), 345 inf (3.08), 361 inf (2.95), 436 inf (3.61) 451 (3.46); ν_{max}/cm^{-1} 1585 m, 1535 s, 1504 m, 1493 m, 1450 m, 1416 m,

1315 m, 1290 m, 1220 m, 1192 m, 1155 m, 1003 m, 910 m, 869 m, 841 m, 818 m, 770 m, 750 m; δ_H (300 MHz, $CDCl_3$) 8.30–8.27 (2H, m, Ar *H*), 7.61–7.57 (5H, m, Ar *H*), 7.47–7.45 (3H, m, Ar *H*), 7.35–7.30 (3H, m, Ar *H*), 7.25–7.23 (2H, m, Ar *H*), 6.95 (1H, s, Ar *H*), 6.10 (1H, s, Ar *H*), 4.84 (2H, br d, *J* 12.6, C*H*$_2$), 3.21 (2H, ddd, *J* 12.3, 12.3, 3.3, C*H*$_2$), 2.93–2.86 (1H, hept, *J* 5.6, C*H*), 2.01–1.43 (4H, m, C*H*$_2$); δ_C (75 MHz, $CDCl_3$) 2 × Ar CH peaks missing, 177.3 (s), 156.0 (s), 153.0 (s), 151.8 (s), 145.1 (s), 141.7 (s), 135.4 (s), 134.8 (s), 129.9 (d), 129.8 (d), 129.7 (d), 128.6 (d), 126.8 (d), 126.5 (d), 125.9 (d), 105.2 (d), 97.6 (d), 50.0 (t), 42.9 (d), 33.5 (t); *m*/*z* (EI) 458 (M^+, 100%), 389 (14), 354 (11), 339 (12), 327 (8), 313 (20), 301 (13), 299 (11), 271 (10), 177 (14), 168 (9), 163 (10), 155 (19), 140 (5), 128 (6), 115 (10), 104 (11), 91 (13), 77 (43), 63 (6). Anal calcd for $C_{30}H_{26}N_4O$ (458.55): C 78.58, H 5.72, N 12.22. Found: C 78.42, H 5.48, N 12.08.

*8.2.9. 6-(4-Benzylpiperazin-1-yl)-1,3-diphenylbenzo[e][1,2,4]triazin-7(1H)-one (**16**)*

Orange needles (16%). Mp: 210–212 °C (from cyclohexane), R_f (Et_2O) 0.18; λ_{max}(DCM)/nm 281 (log ε 3.51), 301 (3.56), 320 inf (3.47), 345 inf (3.16), 432 inf (3.39), 454 (3.47); ν_{max}/cm^{-1} 1537 s, 1315 m, 1296 m, 1231 m, 1204 m, 897 m; δ_H (300 MHz, acetone-d_6) 8.33–8.22 (2H, m, Ar *H*), 7.79–7.61 (5H, m, Ar *H*), 7.53–7.38 (8H, m, Ar *H*), 6.85 (1H, s, Ar *H*), 5.76 (1H, s, Ar *H*), 3.94 (4H, t, *J* 4.2, 2C*H*$_2$), 3.56 (2H, s, C*H*$_2$Ph), 2.61 (4H, t, *J* 4.8, 2C*H*$_2$); δ_C (75 MHz, $CDCl_3$) 177.0 (s), 155.8 (s), 152.9 (s), 151.6 (s), 141.6 (s), 137.5 (s), 135.2 (s), 134.6 (s), 129.8 (d), 129.7 (d), 129.6 (d), 129.1 (d), 128.5 (d), 128.2 (d), 127.2 (d), 126.7 (d), 125.8 (d), 105.3 (d), 97.5 (d), 62.8 (CH_2Ph), 52.8 (t), 48.7 (CH_2); *m*/*z* (EI) 473 (M^+, 21%), 382 (5), 340 (18), 327 (9), 314 (16), 146 (100), 117 (7), 91 (94), 77 (15). Anal calcd for $C_{30}H_{27}N_5O$ (473.57): C 76.09, H 5.75, N 14.79. Found: C 76.03, H 5.62, N 14.69.

*8.2.10. 6-(Azepan-1-yl)-1,3-diphenylbenzo[e][1,2,4]triazin-7(1H)-one (**17**)*

Orange needles (71%). Mp: 191–192°C (aq. EtOH), R_f (Et_2O) 0.42; λ_{max}(DCM)/nm 281 inf (log ε 3.31), 301 (3.43), 324 inf (3.21), 349 inf (2.80), 364 inf (2.71), 456 (3.36); ν_{max}/cm^{-1} 1584 m, 1531 s, 1504 m, 1485 m, 1454 m, 1356 m, 1317 m, 1298 m, 1265 m, 1248 m, 978 m, 905 m, 885 m, 829 m, 820 m, 785 m, 772 m, 745 m; δ_H (300 MHz, $CDCl_3$) 8.28–8.25 (2H, m, Ar *H*), 7.58–7.49 (5H, m, Ar *H*), 7.487.38 (3H, m, Ar *H*), 6.72 (1H, s, Ar *H*), 6.01 (1H, s, Ar *H*), 4.01 (4H, br s, C*H*$_2$N), 1.96–1.88 (4H, br m, C*H*$_2$), 1.65–1.59 (4H, br m, C*H*$_2$); δ_C (75 MHz, $CDCl_3$) 1 Ar CH & 1 CH_2 peaks missing, 177.0 (s), 153.8 (s), 152.5 (s), 152.0 (s), 141.8 (s), 135.7 (s), 134.7 (s), 129.7 (d), 129.5 (d), 128.4 (d), 126.8 (d), 125.9 (d), 101.4 (d), 97.4 (d), 53.3 (t), 26.6 (t); *m*/*z* (EI) 396 (M^+, 100%), 379 (5), 353 (21), 339 (11), 325 (6), 314 (18), 299 (13), 271 (5), 168 (7), 144 (5), 116 (5), 104 (8), 77 (48), 55 (9), 51 (9). Anal calcd for $C_{25}H_{24}N_4O$ (396.48): C 75.73, H 6.10, N 14.13. Found: C 75.90, H 6.13, N 14.06.

*8.2.11. 6-(N-Benzyl-N-methylamino)-1,3-diphenylbenzo[e][1,2,4]triazin-7(1H)-one (**22**)*

Red prisms (38%). Mp: 180–183 °C (from 2-PrOH), R_f (Et_2O) 0.58; λ_{max}(DCM)/nm 277 inf (log ε 3.51), 298 (3.60), 319 inf (3.48), 344 (3.15), 359 inf (3.05), 431 inf (3.45), 450 (3.52); ν_{max}/cm^{-1} 1584 m, 1530 s, 1503 m, 1493 m, 1449 m, 1391 m, 1314 m, 1292 m, 1194 m, 920 m, 818 m, 781 m; δ_H (300 MHz, $CDCl_3$) 8.32–8.22 (2H, m, Ar *H*), 7.65–7.51 (5H, m, Ar *H*), 7.49–7.40 (3H, m, Ar *H*), 7.39–7.23 (5H, m, Ar *H*), 6.76 (1H, s, Ar *H*), 6.09 (1H, s, Ar *H*), 5.33 (2H, s, C*H*$_2$), 3.22 (3H, s, C*H*$_3$); δ_C (75 MHz, $CDCl_3$) 176.8 (s), 154.5 (s), 152.7 (s), 151.8 (s), 141.6 (s), 137.4 (s), 135.4 (s), 134.7 (s), 129.8 (d), 129.7 (d), 129.6 (d), 128.6 (d), 128.4 (d), 127.4 (d), 127.2 (d), 126.7 (d), 125.8 (d), 103.1 (d), 97.4 (d), 56.9 (t), 40.6 (q); *m*/*z* (EI) 418 (M^+, 41%), 403 (23), 327 (100), 209 (10), 180 (10), 91 (16), 77 (30), 65 (6), 51 (6). Anal calcd for $C_{27}H_{22}N_4O$ (418.49): C 77.49, H 5.30, N 13.39. Found: C 77.35, H 5.26, N 13.24.

*8.2.12. 6-(N-Benzyl-N-ethylamino)-1,3-diphenylbenzo[e][1,2,4]triazin-7(1H)-one (**23**)*

Orange prisms (31%). Mp: 180–182 °C (from cyclohexane), R_f (Et_2O) 0.62; λ_{max}(DCM)/nm 299 (log ε 3.66), 320 inf (3.51), 345 (3.17), 360 inf (3.08), 431 inf (3.49), 452 (3.58); ν_{max}/cm^{-1} 1587 m, 1531 s, 1493 m, 1449 m, 1354 m, 1315 s, 1285 m, 1238 m, 970 m, 874 m, 831 m, 779 m; δ_H (300 MHz, acetone-d_6) 8.28–8.21 (2H, m, Ar *H*), 7.78–7.60 (5H, m, Ar *H*), 7.50–7.23 (8H, m, Ar *H*), 6.70 (1H, s, Ar *H*), 5.79 (1H, s, Ar *H*), 5.23 (2H, s, C*H*$_2$), 3.86 (2H, dd, *J* 13.5, 6.5, C*H*$_2$CH$_3$), 1.34 (3H, t, *J* 7.0, CH_2C*H*$_3$); δ_C (75 MHz, $CDCl_3$) 176.8 (s), 153.5 (s), 152.7 (s), 152.0 (s), 141.7 (s), 137.1 (s), 135.5 (s), 134.6 (s), 129.74 (d), 129.69 (d), 129.6 (d), 128.6 (d), 128.4 (d), 127.2 (d), 127.1 (d), 126.8 (d), 125.9 (d), 102.5 (d), 97.5 (d), 54.7 (t), 47.2 (t), 12.5 (q); *m*/*z* (EI) 432 (M^+, 23%), 403 (34), 341 (100), 180 (8), 104 (5), 91 (12), 77 (22), 65 (5). Anal calcd for $C_{28}H_{24}N_4O$ (432.52): C 77.75, H 5.59, N 12.95. Found: C 77.95, H 5.40, N 12.92.

*8.2.13. 6-[8-(N-Benzyl-N-methylamino)octylamino]-1,3-diphenylbenzo[e][1,2,4]triazin-7(1H)-one (**25**)*

Orange needles (59%). Mp: 124–126 °C (from DCM/*n*-pentane), R_f (THF/hexane, 1:1) 0.22; λ_{max}(DCM)/nm 290 (log ε 3.52), 300 (3.52), 314 inf (3.47), 333 (3.12), 414 inf (3.35), 432 (3.44), 488 inf (2.54); ν_{max}/cm^{-1} 1562 s, 1549 s, 1516 m, 1489 s, 1476 s, 1450 m, 1310 m, 1294 m, 773 m; δ_H (300 MHz, $CDCl_3$) 8.35–8.26 (2H, m, Ar *H*), 7.65–7.52 (5H, m, Ar *H*), 7.51–7.41 (3H, m, Ar *H*), 7.36–7.19 (5H, m, Ar *H*), 6.89 (1H, br t, *J* 5.0, N*H*), 6.63 (1H, s, Ar *H*), 6.12 (1H, s, Ar *H*), 3.48 (2H, s, C*H*$_2$Ph), 3.43–3.36 (2H, m, C*H*$_2$), 2.36 (2H, t, *J* 7.5, C*H*$_2$), 2.18 (3H, s, C*H*$_3$), 1.82–1.68 (2H, m, C*H*$_2$), 1.58–1.24 (10H, m, 5C*H*$_2$); δ_C (75 MHz, $CDCl_3$) 1 × CH_2 peak missing, 172.9 (s), 152.4 (s), 152.3 (s), 152.0 (s), 141.8 (s), 139.2 (s), 136.0 (s), 135.4 (s), 130.0 (d), 129.80 (d), 129.76 (d), 129.0 (d), 128.5 (d), 128.1 (d), 126.9 (d), 126.8 (d), 126.0 (d), 95.5 (d), 94.0 (d), 62.3 (t), 57.4 (t), 42.8 (t), 42.2 (q), 29.4 (t), 29.2 (t), 28.5 (t), 27.3 (t), 27.0 (t); *m*/*z* (EI) 545 (M^+, 46%), 454 (19), 424 (7), 327 (7), 315 (5), 134 (21), 91 (100), 77 (9). Anal calcd for $C_{35}H_{39}N_5O$ (545.72): C 77.03, H 7.20, N 12.83. Found: C 76.91, H 7.07, N 12.77.

*8.2.14. 6-[3,4-Dihydroquinolin-1(2H)-yl]-1,3-diphenylbenzo[e][1,2,4]triazin-7(1H)-one (**27**)*

Brown needles (59%). Mp: 213–215°C (from EtOH/cyclohexane), R_f (Et_2O) 0.42; λ_{max}(DCM)/nm 281 (log ε 3.43), 301 (3.55), 325 inf (3.38), 330 inf (3.32), 368 inf (2.74), 451 (3.65); ν_{max}/cm^{-1} 1585 m, 1531 s, 1508 m, 1489 m, 1456 m, 1362 m, 1315 m, 1285 m, 1248 m, 1192 m, 1171 m, 1163 m, 984 m, 870 m, 853 m, 827 m, 781 m, 767 m; δ_H (300 MHz, $CDCl_3$) 8.27–8.25 (2H, m, Ar *H*), 7.66–7.52 (5H, m, Ar *H*), 7.45–.43 (3H, m, Ar *H*), 7.34 (1H, s, Ar *H*), 7.21–7.05 (4H, m, Ar *H*), 6.28 (1H, s, Ar *H*), 4.10 (2H, dd, *J* 5.8, 5.8, C*H*$_2$), 2.88 (2H, t, *J* 6.8, C*H*$_2$), 2.05–1.96 (2H, m, C*H*$_2$); δ_C (75 MHz, $CDCl_3$) 176.9 (s), 155.7 (s), 152.9 (s), 152.0 (s), 141.6 (s), 141.3 (s), 135.1 (s), 134.9 (s), 130.6 (s), 130.1 (d) 130.0 (d), 129.9 (d), 129.6 (d), 128.6 (d), 126.8 (d), 126.3 (d), 125.9 (d), 124.4 (d), 123.3 (d), 112.8 (d), 97.9 (d), 49.1 (t), 26.9 (t), 26.5 (t), 23.6 (t); *m*/*z* (EI) 430 (M^+, 100%), 415 (12), 326 (5), 300 (14), 222 (7), 201 (18), 194 (6), 168 (6), 117 (7), 89 (6), 77 (34), 51 (8). Anal calcd for $C_{28}H_{22}N_4O$ (530.50): C 78.12, H 5.15, N 13.01. Found: C 77.91, H 5.42, N 12.91.

*8.3. Preparation of 5-substituted triazafluoranthenones **32**, **34**–**37***

To a stirred solution of 2-phenyl-6*H*-[1,2,4]triazino[5,6,1-*jk*]carbazol-6-one (**29**) (110 mg, 0.37 mmol) in THF (1 mL) at rt, alkylamine (22.2 mmol) was added. The mixture was stirred at rt for 12 h, then diluted with water (2 mL) and the precipitate that formed filtered, and washed sequentially with water, Et_2O and *n*-pentane. The residue was crystallized to give the product.

*8.3.1. 5-{N-[3-(Dimethylamino)propyl]-N-methylamino}-2-phenyl-6H-[1,2,4]triazino[5,6,1-jk] carbazol-6-one (**32**)*

Orange needles (58%). Mp: 82–86°C (from DCM/MeOH), R_f (DCM/MeOH, 1:5) 0.12; λ_{max}(DCM)/nm 222 (log ε, 3.96), 275 (3.39), 306 (3.27), 413 inf (2.51), 437 (3.12), 460 (3.18); ν_{max}/cm^{-1} 2953 m, 2922 m, 2853 m, 1641 m, 1620 m, 1612 m, 1595 m, 1562 m, 1537 s, 1514 s, 1493 s, 1479 m, 1468 m, 1450 s, 1391 m, 1366 m, 1315 s, 1296 s, 1261 m, 1192 m, 1173 m, 1105 m, 1069 m, 1049 m, 1028 m, 924 m, 822 m, 781 m; δ_H (300 MHz, $CDCl_3$) 8.54–8.49 (2H m, Ar *H*), 8.27 (2H, dd, *J* 8.0, 8.0, Ar *H*), 7.62–7.44 (5H, m, Ar *H*), 6.42 (1H, s, Ar *H*), 4.02 (2H, t, *J* 7.4, C*H*$_2$), 3.35 (3H, s, C*H*$_3$), 2.50 (2H, t, *J* 7.1, C*H*$_2$), 2.34 (6H, s, 2C*H*$_3$), 2.07 (2H, pent, *J* 7.3, C*H*$_2$); δ_C (75 MHz, $CDCl_3$) 174.2 (s), 157.9 (s), 156.7 (s), 152.0 (s), 136.2 (s), 134.8 (s), 130.2 (d), 128.5 (d), 127.7 (d), 127.4 (d), 126.4 (s), 125.2 (s), 124.3 (d), 122.1 (d), 112.9 (d), 104.1 (s), 99.4 (d), 56.7 (t), 53.5 (t), 45.4 (q), 42.2 (q), 26.5 (t); *m*/*z* (EI) 411 (M^+, 2%), 340 (19), 325 (7), 311 (8), 84 (6), 58 (100). Anal calcd for $C_{25}H_{25}N_5O$ (411.50): C 72.97, H 6.12, N 17.02. Found: C 72.90, H 6.19, N 16.92.

*8.3.2. 5-(3-Methylpiperidin-1-yl)-2-phenyl-6H-[1,2,4]triazino[5,6,1-jk]carbazol-6-one (**34**)*

Red prisms (45%). Mp: 151–154 °C (from cyclohexane), R_f (Et_2O) 0.73; λ_{max}(DCM)/nm 235 (log ε 3.62), 270 inf (3.65), 280 (3.66), 306 (3.52), 363 (2.83), 380 (2.83), 413 inf (3.07), 441 (3.42), 466 (3.54), 527 inf (2.70); ν_{max}/cm^{-1} 1641 m, 1620 s, 1524 s, 1514 s, 1479 m, 1452 m, 1391 m, 1369 m, 1317 m, 1258 m, 1234 s, 1138 m, 1126 m, 943 m, 853 m, 797 m; δ_H (500 MHz, $CDCl_3$) 8.49 (2H, d, *J* 7.4, Ar *H*), 8.30 (1H, d, *J* 8.0, Ar *H*), 8.27 (1H, d, *J* 8.0, Ar *H*), 7.61–7.47 (5H, m, Ar *H*), 6.61 (1H, s, Ar *H*), 4.53 (1H, br d, *J* 11.2, C*H*$_2$), 4.43 (1H, br d, *J* 12.0, C*H*$_2$), 3.16 (1H, t, *J* 13.6, C*H*$_2$), 2.87 (1H, t, *J* 11.7, C*H*$_2$), 2.01–1.77 (4H, m, Ar *H*), 1.34–1.23 (1H, m, C*H*), 1.01 (3H, d, *J* 6.3, C*H*$_3$); δ_C (75 MHz, $CDCl_3$) 1 × Ar CH peak missing, 174.6 (s), 160.2 (s), 156.8 (s), 152.5 (s), 136.2 (s), 134.9 (s), 130.3 (d), 128.6 (d), 127.8 (d), 126.6 (s), 125.3 (s), 124.5 (d), 122.3 (d), 113.1 (d), 104.5 (s), 102.9 (d), 58.0 (t), 51.2 (t), 33.1 (t), 31.7 (d), 25.7 (t) 19.2 (q); *m*/*z* (EI) 394 (M^+, 100%), 351 (10), 339 (14), 325 (10), 312 (18), 297 (20), 285 (5), 269 (6), 197 (8), 139 (5), 98 (13), 84 (9). Anal calcd for $C_{25}H_{22}N_4O$ (394.47): C 76.12, H 5.62, N 14.20. Found: C 76.28, H 5.71, N 14.18.

*8.3.3. 2-Phenyl-5-(4-phenylpiperidin-1-yl)-6H-[1,2,4]triazino[5,6,1-jk]carbazol-6-one (**35**)*

Red prisms (79%). Mp: 171–173 °C (from cyclohexane), R_f (Et_2O) 0.73; λ_{max}(DCM)/nm 234 (log ε 3.63), 260 inf (3.61), 273 (3.65), 280 (3.66), 305 (3.53), 362 (2.79), 383 (2.84), 413 inf (3.11), 440 (3.43), 464 (3.54); ν_{max}/cm^{-1} 1641 m, 1624 s, 1524 s, 1514 s, 1481 m, 1452 m, 1443 m, 1433 m, 1393 m, 1312 m, 1258 m, 1209 s, 1179 m, 1099 m, 1009 m, 945 m, 827 m, 795 m; δ_H (500 MHz, $CDCl_3$) 8.51 (2H, d, *J* 8.0, Ar *H*), 8.31 (1H, d, *J* 8.0, Ar *H*), 8.28 (1H, d, *J* 8.5, Ar *H*), 7.62–7.49 (5H, m, Ar *H*), 7.39–7.31 (2H, m, Ar *H*), 7.29–7.22 (3H, m, Ar *H*), 6.69 (1H, s, Ar *H*), 4.77–4.67 (2H, m, C*H*$_2$), 3.32–3.23 (2H, m, C*H*$_2$), 2.96–2.87 (1H, m, C*H*), 2.11–2.00 (4H, m, C*H*$_2$); δ_C (125 MHz, $CDCl_3$) 1 × Ar CH peak missing, 174.5 (s), 160.3 (s), 156.7 (s), 152.4 (s), 145.0 (s), 136.0 (s), 134.8 (s), 130.4 (d), 128.6 (d), 127.8 (d), 127.7 (d), 126.8 (d), 126.6 (s), 126.5 (d), 125.1 (s), 124.6 (d), 122.2 (d), 113.1 (d), 104.5 (s), 103.6 (d), 51.1 (t), 42.6 (d), 33.5 (t); *m*/*z* (EI) 456 (M^+, 100%), 387 (7), 352 (12), 337 (12), 325 (8), 311 (37), 297 (13), 269 (5), 176 (17), 162 (13), 115 (7), 77 (5), 56 (5). Anal calcd for $C_{30}H_{24}N_4O$ (456.54): C 78.92, H 5.30, N 12.27. Found: C 79.06, H 5.48, N 12.26.

*8.3.4. 5-(N-Benzyl-N-methylamino)-2-phenyl-6H-[1,2,4]triazino[5,6,1-jk]carbazol-6-one (**36**)*

Red prisms (21%), Mp: 153–155 °C (from cyclohexane), R_f (Et_2O) 0.69; λ_{max}(DCM)/nm 233 (log ε 3.65), 260 inf (3.66), 271 (3.70), 279 (3.69), 306 (3.54), 363 (2.82), 379 (2.84), 409 inf (3.08), 435 (3.44), 459 (3.58), 525 inf (2.52); ν_{max}/cm^{-1} 1645 m, 1622 m, 1614 m, 1514 s, 1481 m, 1452 m, 1391 m, 1314 m, 1261 m, 1229 m, 1190 m, 1109 m, 945 m, 901 m, 789 m, 752 m; δ_H (300 MHz, $CDCl_3$) 8.53–8.47 (2H, m, Ar *H*), 8.30 (2H, dd, *J* 9.0, 7.9, Ar *H*), 7.62–7.47 (5H, m, Ar *H*), 7.42–7.27 (5H, m, Ar *H*), 6.52 (1H, s, Ar *H*), 5.28 (2H, s, C*H*$_2$), 3.27 (3H, s, C*H*$_3$); δ_C (75 MHz, $CDCl_3$) 1 × Ar CH peak missing, 174.3 (s), 158.6 (s), 156.8 (s), 152.3 (s), 137.1 (s), 136.1 (s), 134.9 (s), 130.3 (d), 128.7 (d), 128.6 (d), 127.8 (d), 127.5 (d), 127.3 (d), 126.5 (s), 125.2 (s), 124.6 (d), 122.3 (d), 113.0 (d), 104.3 (s), 101.0 (d), 58.0 (t), 41.5 (q); *m*/*z* (EI) 416 (M^+, 50%), 401 (10), 325 (100), 256 (6), 208 (8), 151 (5), 140 (6), 125 (5), 118 (6), 105 (7), 91 (12), 77 (10). Anal calcd for $C_{27}H_{20}N_4O$ (416.47): C 77.87, H 4.84, N 13.45. Found: C 77.77, H 4.68, N 13.37.

*8.3.5. 5-({8-[Benzyl(methyl)amino]octyl}amino)-2-phenyl-6H-[1,2,4]triazino[5,6,1-jk]-carbazol-6-one (**37**)*

Orange prisms (51%). Mp: 148–149 °C (from DCM/*n*-pentane), R_f (THF/hexane, 1:1) 0.31; λ_{max}(DCM)/nm 231 (log ε 3.59), 256 inf (3.57), 267 (3.62), 276 (3.65), 304 (3.54), 312 inf (3,53), 353 (2.85), 368 (2.84), 394 inf (3.0), 417 (3.40), 440 (3,58), 466 inf (2.62); ν_{max}/cm^{-1} 1638 m, 1555 s, 1526 s, 1493 m, 1472 s, 1454 m, 1319 m, 1306 m; δ_H (300 MHz, $CDCl_3$) 8.52 (2H, d, *J* 7.8, Ar *H*), 8.28 (2H, d, *J* 7.8, Ar *H*), 7.65–7.47 (5H, m, Ar *H*), 7.36–7.20 (5H, m, Ar *H*), 7.09 (1H, t, *J* 4.8, N*H*), 6.31 (1H, s, Ar *H*), 3.49 (2H, s, C*H*$_2$Ph), 3.46–3.36 (2H, m, C*H*$_2$), 2.42–2.31 (2H, m, NHC*H*$_2$), 2.18 (3H, s, C*H*$_3$), 1.87–1.73 (2H, m, NC*H*$_2$), 1.59–1.27 (10H, m, 5C*H*$_2$); δ_C (75 MHz, $CDCl_3$) 1 × Cq peak missing, 170.5 (s), 157.1 (s), 155.0 (s), 152.7 (s), 136.1 (s), 135.6 (s), 130.4 (d), 129.1 (d), 128.7 (d), 128.2 (d), 128.1 (d), 127.9 (d), 126.9 (d), 126.34 (s), 126.31 (s), 124.8 (d), 122.4 (d), 113.3 (d), 102.2 (s), 92.6 (d), 62.3 (t), 57.4 (t), 43.5 (t), 42.2 (q), 29.4 (t), 29.2 (t), 28.4 (t), 27.31 (t), 27.28 (t), 27.1 (t); *m*/*z* (EI) 543 (M^+, 38%), 452 (25), 134 (48), 91 (100). Anal calcd for $C_{35}H_{37}N_5O$ (543.70): C 77.32, H 6.86, N 12.88. Found: C 77.26, H 6.97, N 12.76.

*8.4. Preparation of N-[(N-benzyl-N-methylamino)alkyl]-N-methylamino substituted benzotriazinones **24** and **26** and triazafluoranthenone **38***

*8.4.1. General procedure for the preparation of 6-methylaminobenzotriazinones **40** and **41***

To a stirred solution of 1,3-diphenylbenzo[*e*][1,2,4]triazin-7(1*H*)-one (**1**) or 8-iodo-1,3-diphenylbenzo[*e*][1,2,4]triazin-7(1*H*)-one (**39**) [22] (0.27 mmol) in THF (2 mL), methylamine (0.4 mL, 40% aq. soln) was added. The mixture was stirred at rt for 30 min. The mixture was diluted with water (2 mL) and the precipitate was collected by filtration, washed sequentially with water, Et_2O and *n*-pentane. Crystallization of the residue gave the product.

*8.4.1.1. 6-(Methylamino)-1,3-diphenylbenzo[e][1,2,4]triazin-7(1H)-one (**40**).* Orange needles (84%). Mp: 307–311 °C (from $CHCl_3$), R_f (THF/hexane, 1:1) 0.24; λ_{max}(DCM)/nm 247 inf (log ε 3.20), 276 inf (3.46), 288 (3.49), 300 (3.49), 313 inf (3.46), 332 inf (3.14), 350 inf (3.04), 409 inf (3.31), 430 (3.40), 496 inf (2.50), 535 inf (2.22); ν_{max}/cm^{-1} 1547 s, 1491 s, 1477 s, 1449 m, 1416 m, 1396 m, 1383 m, 1314 s, 1298 m, 1279 m, 988 m, 858 m, 812 m, 781 m, 752w; δ_H (300 MHz, $CDCl_3$) 8.35–8.26 (2H, m, Ar *H*), 7.65–7.53 (5H, m, Ar *H*), 7.52–7.42 (3H, m, Ar *H*), 6.89 (1H, br s, N*H*), 6.62 (1H, s, Ar *H*), 6.11 (1H, s, Ar *H*), 3.13 (3H, d, *J* 5.5, C*H*$_3$); δ_C (75 MHz, $CDCl_3$) 173.0 (s), 153.0 (s), 152.5 (s), 152.4 (s), 141.8 (s), 136.1 (s), 135.3 (s), 130.1 (d), 129.9 (d), 129.8 (d), 128.6 (d), 127.0 (d), 126.0 (d), 95.5 (d), 94.0 (d), 29.4 (q); *m*/*z* (EI) 328 (M^+, 100%), 300 (18), 168 (5), 164 (5), 120 (9), 104 (5), 77 (37), 51 (14). Anal calcd for $C_{20}H_{16}N_4O$ (328.37): C 73.15, H 4.91, N 17.06. Found: C 73.08, H 4.80, N 16.90.

*8.4.1.2. 8-Iodo-6-(methylamino)-1,3-diphenylbenzo[e][1,2,4]triazin-7(1H)-one (**41**).* Red needles (70%). Mp: 294–296 °C (from $CHCl_3$), R_f (Et_2O) 0.38; λ_{max}(DCM)/nm 256 (log ε 3.43), 300 (3.56), 349 inf

(3.29), 419 inf (3.37), 437 (3.44), 514 inf (2.57); ν_{max}/cm^{-1} 1574 s, 1510 m, 1460 s, 1447 s, 1416 s, 1308 m, 901 m, 781 m; δ_H (500 MHz, $CDCl_3$) 8.34–8.28 (2H, m, Ar *H*), 7.59–7.43 (8H, m, Ar *H*), 6.89 (1H, br s, N*H*), 6.58 (1H, s, Ar *H*), 3.14 (3H, d, *J* 5.5, CH_3); δ_C (125 MHz, $CDCl_3$) 171.5 (s), 154.1 (s), 151.7 (s), 149.7 (s), 142.8 (s), 137.3 (s), 134.6 (s), 130.3 (d), 129.3 (d), 129.1 (d), 128.6 (d), 127.4 (d), 127.0 (d), 95.5 (d), 68.3 (s), 29.6 (q); *m*/*z* (EI) 454 (M^+, 47%), 327 (100), 312 (7), 299 (7), 284 (17), 181 (7), 168 (5), 155 (10), 149 (14), 140 (5), 127 (7), 116 (10), 91 (5), 77 (30), 51 (9). Anal calcd for $C_{20}H_{15}IN_4O$ (454.26): C 52.88, H 3.33, N 12.33. Found: C 53.02, H 3.24, N 12.28.

8.4.2. General procedure for the preparation of 6-(N-bromoalkyl-N-methylamino) substituted benzotriazinones ***42–44***

To a stirred solution of either 6-(methylamino)-1,3-diphenylbenzo[*e*][1,2,4]triazin-7(1*H*)-one (**40**) or 8-iodo-6-(methylamino)-1,3-diphenylbenzo[*e*][1,2,4]triazin-7(1*H*)-one (**41**) (0.31 mmol) in dry DMF (2 mL) at rt, NaH 60% dispersion in mineral oil, (15 mg, 0.36 mmol) was added. The mixture was stirred at rt for 30 min and then dibromoalkane (0.91 mmol) was added and the mixture was stirred for a further 12 h. The reaction mixture was then diluted with DCM (20 mL) and washed with water (2 × 20 mL). The organic layer was separated, dried (Na_2SO_4), filtered and the volatiles removed. The residue was then dissolved in DCM (5 mL), adsorbed onto silica and chromatographed (hexane) to remove excess of dibromoalkane, and then with *t*-BuOMe to give the product.

*8.4.2.1. 6-[N-(5-Bromopentyl)-N-methylamino]-1,3-diphenylbenzo[e][1,2,4]triazin-7(1H)-one (**42**).* Red needles (54%). Mp: 137–139 °C (DCM/*n*-pentane), R_f (Et_2O) 0.51; λ_{max}(DCM)/nm 280 inf (log ε 3.44), 300 (3.62), 320 inf (3.47), 345 (3.09), 361 inf (3.0), 431 inf (3.45), 453 (3.55); ν_{max}/cm^{-1} 1587 m, 1535 s, 1499 m, 1450 m, 1314 m, 1298 m, 1256 m, 827 m, 772 m; δ_H (300 MHz, $CDCl_3$) 8.32–8.23 (2H, m, Ar *H*), 7.64–7.50 (5H, m, Ar *H*), 7.50–7.40 (3H, m, Ar *H*), 6.67 (1H, s, Ar *H*), 6.02 (1H, s, Ar *H*), 4.00 (2H, br t, *J* 6.3, CH_2), 3.43 (2H, t, *J* 6.6, CH_2), 3.30 (3H, s, CH_3), 1.92 (2H, pent, *J* 6.8, CH_2), 1.77 (2H, pent, *J* 7.5, CH_2), 1.50 (2H, pent, *J* 7.4, CH_2); δ_C (75 MHz, $CDCl_3$) 176.8 (s), 154.2 (s), 152.5 (s), 151.9 (s), 141.7 (s), 135.5 (s), 134.7 (s), 129.8 (d), 129.7 (d), 129.5 (d), 128.5 (d), 126.8 (d), 125.9 (d), 102.0 (d), 97.3 (d), 54.2 (t), 41.3 (q), 33.6 (t), 32.2 (t), 27.7 (t), 25.3 (t); *m*/*z* (EI) 478 ($M^+ + 2$, 70%), 476 (M^+, 78), 463 (32), 461 (33), 397 (10), 368 (18), 355 (28), 341 (81), 327 (90), 313 (40), 299 (27), 285 (8), 271 (14), 195 (6), 180 (25), 170 (26), 140 (11), 132 (16), 116 (12), 94 (10), 90 (10), 77 (100), 69 (7), 64 (9), 55 (11), 51 (16). Anal calcd for $C_{25}H_{25}BrN_4O$ (477.40): C 62.90, H 5.28, N 11.74. Found: C 63.04, H 5.19, N 11.90.

*8.4.2.2. 6-[N-(8-Bromooctyl)-N-methylamino]-1,3-diphenylbenzo[e][1,2,4]triazin-7(1H)-one (**43**).* Red prisms (73%). Mp: 87–88 °C (from DCM/*n*-pentane), R_f (Et_2O) 0.62; λ_{max}(DCM)/nm 278 inf (log ε 3.57), 300 (3.67), 320 inf (3.52), 345 (3.12), 362 inf (3.03), 431 inf (3.49), 453 (3.59); ν_{max}/cm^{-1} 1595 m, 1537 s, 1315 m, 1296 m; δ_H (300 MHz, $CDCl_3$) 8.27 (2H, dd, *J* 7.3, 2.3, Ar *H*), 7.63–7.51 (5H, m, Ar *H*), 7.49–7.41 (3H, m, Ar *H*), 6.67 (1H, s, Ar *H*), 6.02 (1H, s, Ar *H*), 3.96 (2H, br pent, *J* 4.9, CH_2), 3.40 (2H, t, *J* 6.8, CH_2), 3.32 (3H, br s, CH_3), 1.85 (2H, pent, *J* 6.8, CH_2), 1.73 (2H, br pent, *J* 6.8, CH_2), 1.49–1.25 (8H, m, CH_2); δ_C (75 MHz, $CDCl_3$) 176.9 (s), 154.2 (s), 152.5 (s), 152.0 (s), 141.7 (s), 135.6 (s), 134.8 (s), 129.73 (d), 129.66 (d), 129.5 (d), 128.5 (d), 126.8 (d), 125.9 (d), 101.9 (d), 97.3 (d), 54.6 (t), 41.3 (q), 33.9 (t), 32.7 (t), 29.1 (t), 28.6 (t), 28.3 (t), 28.0 (t), 26.7 (t); *m*/*z* (EI) 520 ($M^+ + 2$, 100%), 518 (M^+, 98), 505 (27), 503 (32), 491 (7), 438 (10), 423 (14), 355 (29), 341 (88), 327 (78), 313 (37), 299 (14), 285 (7), 271 (7), 184 (10), 180 (18), 171 (23), 168 (9), 144 (7), 132 (8), 116 (7), 104 (9), 91 (7), 77 (46), 67 (6), 55 (14). Anal calcd for $C_{28}H_{31}BrN_4O$ (519.48): C 64.74, H 6.01, N 10.79. Found: C 64.56, H 5.87, N 10.64.

*8.4.2.3. 6-[N-(8-Bromooctyl)-N-methylamino]-8-iodo-1,3-diphenylbenzo[e][1,2,4]triazin-7(1H)-one (**44**).* Orange prisms (61%). Mp: 97–99 °C (from cyclohexane/*n*-pentane), R_f (Et_2O) 0.71; λ_{max}(DCM)/nm 247 (log ε 3.50), 276 (3.47), 310 (3.65), 363 inf (3.24), 461 (3.59); ν_{max}/cm^{-1} 1562 s, 1530 m, 1487 s, 1474 s, 1454 m, 1443 m, 1404 m, 1364 m, 1312 m, 1290 s, 818 m, 770 m; δ_H (500 MHz, $CDCl_3$) 8.30–8.25 (2H, m, Ar *H*), 7.56–7.51 (4H, m, Ar *H*), 7.50–7.42 (4H, m, Ar *H*), 6.63 (1H, s, Ar *H*), 3.84 (2H, br s, CH_2), 3.41 (2H, t, *J* 6.8, CH_2), 3.34 (3H, br s, CH_3), 1.86 (2H, pent, *J* 6.9, CH_2), 1.78 (2H, br t, *J* 6.8, CH_2), 1.48–1.40 (2H, m, CH_2), 1.40–1.27 (6H, m, CH_2); δ_C (125 MHz, $CDCl_3$) 173.0 (s), 153.7 (s), 151.6 (s), 151.2 (s), 142.7 (s), 137.3 (s), 134.8 (s), 130.0 (d), 129.0 (d), 128.9 (d), 128.5 (d), 127.0 (d), 126.9 (d), 100.8 (d), 73.9 (s), 55.1 (t), 41.3 (q), 33.9 (t), 32.7 (t), 29.2 (t), 28.6 (t), 28.0 (t), 26.8 (t), 26.7 (t); *m*/*z* (EI) 646 ($M^+ + 2$, 99%), 644 (M^+, 100), 631 (14), 629 (15), 518 (12), 481 (10), 467 (34), 453 (24), 439 (9), 339 (13), 327 (29), 313 (15), 298 (31), 284 (7), 234 (15), 208 (7), 180 (21), 170 (16), 156 (7), 140 (11), 128 (8), 116 (8), 104 (9), 77 (44), 69 (7). Anal calcd for $C_{28}H_{30}BrIN_4O$ (645.37): C 52.11, H 4.69, N 8.68. Found: C 51.98, H 4.53, N 8.75.

*8.4.3. Preparation of 5-[N-(8-bromooctyl)-N-methylamino]-2-phenyl-6H-[1,2,4]triazino[5,6,1-jk]carbazol-6-one (**45**)*

To a stirred solution of 6-[*N*-(5-bromooctyl)-*N*-methylamino]-8-iodo-1,3-diphenylbenzo[*e*] [1,2,4]triazin-7(1*H*)-one (**44**) (0.17 mmol) in DMF (1 mL) at rt, were added $Pd(Ph_3P)_2Cl_2$ (11 mg, 0.016 mmol, 10 mol %) and AgF (32 mg, 0.25 mmol), and the mixture was heated at ca. 100 °C for 1 h. The reaction mixture was allowed to cool to rt and then diluted with Et_2O (5 mL) and washed with H_2O (5 mL). The organic layer was separated, dried (Na_2SO_4), filtered and evaporated in vacuo. Chromatography (DCM) of the residue gave the title compound **45** as red prisms (39%). Mp: 72–73 °C (from cyclohexane/*n*-pentane), R_f (Et_2O) 0.71; λ_{max}(DCM)/nm 233 (log ε 3.57), 275 (3.69), 305 inf (3.53), 363 (2.61), 412 inf (3.12), 437 (3.40), 460 (3.48); ν_{max}/cm^{-1} 1645 m, 1628 m, 1535 s, 1514 s, 1479 m, 1450 m, 1391 m, 1310 m, 1261 m, 787 m, 752 m; δ_H (300 MHz, $CDCl_3$) 8.46 (2H, dd, *J* 2.1, 7.5, Ar *H*), 8.25 (1H, d, *J* 7.7, Ar *H*), 8.20 (1H, d, *J* 8.1, Ar *H*), 7.58–7.41 (5H, m, Ar *H*), 6.32 (1H, s, Ar *H*), 3.90 (2H, br t, *J* 7.0, CH_2), 3.41 (2H, t, *J* 6.8, CH_2), 3.32 (3H, s, CH_3), 1.92–1.73 (4H, m, 2CH_2), 1.52–1.29 (8H, m, 4CH_2); δ_C (75 MHz, $CDCl_3$) 174.4 (s), 158.0 (s), 156.9 (s), 152.1 (s), 136.3 (s), 134.9 (s), 130.2 (d), 128.5 (d), 127.8 (d), 127.7 (d), 126.5 (s), 125.4 (s), 124.4 (d), 122.2 (d), 113.0 (d), 104.2 (s), 99.4 (d), 55.5 (t), 42.3 (q), 34.0 (t), 32.7 (t), 29.2 (t), 28.7 (t), 28.3 (t), 28.1 (t), 26.8 (t); *m*/*z* (EI) 518 ($M^+ + 2$, 86%), 518 (M^+, 87), 503 (15), 501 (15), 353 (11), 339 (100), 325 (44), 311 (27), 297 (22), 282 (7), 269 (7), 256 (6), 220 (6), 183 (7), 169 (55), 151 (6), 140 (14), 125 (6), 115 (6), 77 (8), 67 (7), 55 (26). Anal calcd for $C_{28}H_{29}BrN_4O$ (517.46): C 64.99, H 5.65, N 10.83. Found: C 64.84, H 5.56, N 10.74.

8.4.4. General procedure for the preparation of N-[5-(N-benzyl-N-methylamino)alkyl]-N-methylamino substituted benzotriazinones ***24*** *and* ***26*** *and triazafluoranthenone* ***38***

To a stirred solution of 6-[*N*-(bromoalkyl)-*N*-methylamino]-1,3-diphenylbenzo[*e*][1,2,4]triazin-7(1*H*)-ones **42** or **43**, or 5-[*N*-(8-bromooctyl)-*N*-methylamino]-2-phenyl-6*H*-[1,2,4]triazino[5,6,1-*jk*]-carbazol-6-one (**45**) (0.11 mmol) in toluene (5 mL) at rt, *N*-methylbenzylamine (25 mg, 0.21 mmol) was added. The mixture was heated at *ca.* 110 °C for 12 h and allowed to cool to rt, diluted with DCM (15 mL), washed with water (2 × 20 mL), dried (Na_2SO_4), filtered and the volatiles evaporated in vacuo. The residue was then dissolved in DCM (5 mL), adsorbed onto silica and chromatographed (DCM) to remove traces of amine, and then further elution with THF gave the product.

*8.4.4.1. 6-{N-[5-(N-Benzyl-N-methylamino)pentyl]-N-methylamino}-1,3-diphenylbenzo[e] [1,2,4]triazin-7(1H)-one (**24**).* Orange needles (30%). Mp: 88–90 °C (from 2-PrOH/*n*-pentane), R_f (THF/hexane, 1:1)

0.16; λ_{max}(DCM)/nm 279 inf (log ε 3.47), 300 (3.57), 318 inf (3.44), 346 (3.01), 361 (2.94), 431 inf (3.39), 453 (3.50); ν_{max}/cm^{-1} 1595 m, 1537 s, 1485 m, 1450 m, 1315 m, 1298 m, 822 m, 779 m; δ_H (300 MHz, $CDCl_3$) 8.32–8.24 (2H, m, Ar *H*), 7.64–7.50 (5H, m, Ar *H*), 7.49–7.41 (3H, m, Ar *H*), 7.34–7.19 (5H, m, Ar *H*), 6.66 (1H, s, Ar *H*), 6.01 (1H, s, Ar *H*), 3.95 (2H, br s, C*H*$_2$), 3.46 (2H, s, C*H*$_2$), 3.31 (3H, br s, C*H*$_3$), 2.37 (2H, t, *J* 7.3, C*H*$_2$), 2.18 (3H, s, C*H*$_3$), 1.73 (2H, pent, *J* 7.5, C*H*$_2$), 1.55 (2H, pent, *J* 7.5, C*H*$_2$), 1.35 (2H, pent, *J* 7.3, C*H*$_2$); δ_C (75 MHz, $CDCl_3$) 1 × Ar CH peak missing, 176.9 (s), 154.2 (s), 152.5 (s), 151.9 (s), 141.7 (s), 139.2 (s), 135.6 (s), 134.7 (s), 129.7 (d), 129.6 (d), 129.5 (d), 128.9 (d), 128.4 (d), 128.1 (d), 126.8 (d), 125.9 (d), 101.9 (d), 97.3 (d), 62.3 (t), 57.2 (t), 54.5 (t), 42.2 (q), 41.3 (q), 28.2 (t), 27.1 (t), 24.6 (t); *m*/*z* (EI) 517 (M^+, 84%), 396 (14), 381 (8), 341 (11), 329 (43), 313 (7), 300 (5), 292 (5), 188 (10), 180 (8), 160 (10), 134 (16), 120 (7), 98 (84), 91 (100), 77 (21), 70 (10), 65 (7). Anal calcd for $C_{33}H_{35}N_5O$ (517.66): C 76.57, H 6.81, N 13.53. Found: C 76.44, H 7.00, N 13.54.

*8.4.4.2. 6-{N-[8-(N-Benzyl-N-methylamino)octyl]-N-methylamino}-1,3-diphenylbenzo[e] [1,2,4]triazin-7(1H)-one (**26**).* Orange needles (32%). Mp: 97–99 °C (from 2-PrOH), R_f (THF/hexane, 1:1) 0.20; λ_{max}(DCM)/nm 276 inf (log ε 3.46), 300 (3.57), 346 (3.04), 363 inf (2.94), 433 inf (3.40), 454 (3.47); ν_{max}/cm^{-1} 1589 m, 1537 s, 1450 m, 1315 m, 1296 m, 1285 m, 820 m; δ_H (500 MHz, $CDCl_3$) 8.27 (2H, d, *J* 6.8, Ar *H*), 7.62–7.50 (5H, m, Ar *H*), 7.48–7.40 (3H, m, Ar *H*), 7.33–7.20 (5H, m, Ar *H*), 6.66 (1H, s, Ar *H*), 6.02 (1H, s, Ar *H*), 3.99–3.88 (2H, m, C*H*$_2$), 3.46 (2H, s, C*H*$_2$Ph), 3.33 (3H, br s, C*H*$_3$), 2.34 (2H, t, *J* 7.3, C*H*$_2$), 2.17 (3H, s, C*H*$_3$), 1.76–1.67 (2H, m, C*H*$_2$), 1.53–1.46 (2H, m, C*H*$_2$), 1.38–1.34 (8H, m, 4C*H*$_2$); δ_C (125 MHz, $CDCl_3$) 1 × Ar CH and 1 × CH_2 missing, 176.9 (s), 154.3 (s), 152.5 (s), 152.0 (s), 141.8 (s), 139.3 (s), 135.6 (s), 134.8 (s), 129.73 (d), 129.67 (d), 129.5 (d), 129.0 (d), 128.5 (d), 128.1 (d), 126.8 (d), 125.9 (d), 101.9 (d), 97.3 (d), 62.3 (t), 57.5 (t), 54.7 (t), 42.2 (q), 41.3 (q), 29.5 (t), 29.4 (t), 27.4 (t), 27.3 (t), 26.8 (t); *m*/*z* (EI) 559 (M^+, 73%), 468 (10), 341 (8), 329 (12), 250 (7), 238 (5), 180 (6), 169 (6), 154 (5), 147 (6), 140 (9), 134 (17), 120 (5), 108 (6), 91 (92), 77 (15), 65 (6), 57 (5). Anal calcd for $C_{36}H_{41}N_5O$ (559.74): C 77.25, H 7.38, N 12.51. Found: C 77.35, H 7.28, N 12.52.

*8.4.4.3. 5-{N-[8-(N-Benzyl-N-methylamino)octyl]-N-methylamino}-2-phenyl-6H-[1,2,4]-triazino[5,6,1-jk]carbazol-6-one (**38**).* Red prisms (90%). Mp: 56–57 °C (from hexane), R_f (THF/hexane, 1:1) 0.31; λ_{max}(DCM)/nm 234 (log ε 3.57), 274 (3.71), 302 inf (3.53), 369 (2.78), 409 inf (3.02), 437 (3.38), 460 (3.45); ν_{max}/cm^{-1} 1645 s, 1626 m, 1537 s, 1514 s, 1479 m, 1452 m, 1389 m, 1310 m, 1265 s, 783 m, 754 m; δ_H (300 MHz, $CDCl_3$) 8.54–8.44 (2H, m, Ar *H*), 8.32–8.22 (2H, m, Ar *H*), 7.61–7.45 (5H, m, Ar *H*), 7.37–7.19 (5H, m, Ar *H*), 6.39 (1H, s, Ar *H*), 3.93 (2H, br t, *J* 7.4, C*H*$_2$), 3.48 (2H, s, C*H*$_2$), 3.37 (3H, s, C*H*$_3$), 2.36 (2H, t, *J* 7.2, C*H*$_2$), 2.18 (3H, s, C*H*$_3$), 1.98–1.76 (4H, m, 2C*H*$_2$), 1.42–1.28 (8H, m, 4C*H*$_2$); δ_C (75 MHz, $CDCl_3$) 174.5 (s), 158.1 (s), 157.0 (s), 152.2 (s), 138.9 (s), 136.3 (s), 135.0 (s), 130.2 (d), 129.1 (d), 128.6 (d), 128.2 (d), 127.8 (d), 127.7 (d), 126.9 (d), 126.6 (s), 125.5 (s), 124.4 (d), 122.3 (d), 113.1 (d), 104.3 (s), 99.4 (d), 62.2 (t), 57.4 (t), 55.7 (t), 42.3 (q), 42.1 (q), 29.7 (t), 29.4 (t), 28.3 (t), 27.4 (t), 27.2 (t), 26.9 (t); *m*/*z* (EI) 557 (M^+, 56%), 466 (9), 339 (21), 327 (20), 298 (5), 160 (14), 154 (16), 147 (5), 140 (9), 134 (47), 120 (7), 91 (100). Anal calcd for $C_{36}H_{39}N_5O$ (557.73): C 77.53, H 7.05, N 12.56. Found: C 77.65, H 7.17, N 12.49.

8.5. Thioflavin T fluorescence spectroscopy analysis

A known spectrofluorimetric method [14–16], based on fluorescence emission of ThT, was followed. To obtain batches of $A\beta_{1-40}$ and $A\beta_{1-42}$ free from preaggregates, commercial peptides (purity >95%; EzBiolab, Carmel, USA) were dissolved in HFIP, lyophilized and stored at 20 °C. The solution of ThT (25 μM) used for fluorimetric measures was prepared in phosphate buffer 0.025 M, pH 6.0, filtered through 0.45 μm nylon filters and stored at 4 °C. For $A\beta_{1-40}$ inhibition, compounds were first tested at 100 μM; test samples were prepared in phosphate buffered saline (PBS; 0.01 M, NaCl 0.1 M, pH 7.4), with 30 μM Aβ peptide concentration, and contained 2% HFIP and 10% DMSO. Blank samples were prepared for each concentration, devoid of peptide, and their fluorescence value subtracted from the corresponding fluorescence values of coincubation samples. As the control, a sample of peptide was incubated in the same PBS/2% HFIP/10% DMSO buffer, without inhibitor. Incubations were run in triplicate at 25 °C for 2 h. Fluorimetric measures were performed in a 700 μL cuvette with a Perkin–Elmer LS55 spectrofluorimeter, using FLWinlab program. 470 μL of ThT solution were mixed with 30 μL of sample, and the resulting fluorescence measured with parameters set as follows: excitation at 440 nm (slit 5 nm); emission at 485 nm (slit 10 nm); integration time 2 s. Biological activity was determined as percent of inhibitory activity V_i for each concentration, according to the formula:

$$V_i = 100 - [(F_i - F_b)/F_0] \times 100$$

where F_i is the fluorescence value of the sample, F_b its blank value, and F_0 the fluorescence value of Aβ control (already subtracted of its blank). For the most active inhibitors, IC_{50} values were determined by testing in duplicate 5–7 concentrations, ranging from 200 to 0.01 μM. Statistics from three independent experiments were calculated within GraphPad Prism® v. 5 software.

Inhibition test of $A\beta_{1-42}$ was performed according to a previous method [37] with modifications. $A\beta_{1-42}$ (30 μM) was incubated in PBS/10% DMSO at 37 °C alone as control and with selected compounds (100 μM); spectrofluorimetric lectures with ThT were performed as above described for $A\beta_{1-40}$ at 8 h and 24 h time points. Fluorescence values are reported as arbitrary units in the graph of Fig. 4, obtained as the mean ± SEM from three independent experiments and calculated within GraphPad Prism software.

8.6. Inhibition of cholinesterases

The in vitro inhibition assays of AChE from electric eel (463 U/mg) and BChE from equine serum (13 U/mg) were run in phosphate buffer 0.1 M, pH 8.0. Acetyl- and butyrylthiocholine iodides were used, respectively, as substrates, and 5,5′-dithiobis(2-nitrobenzoic acid) (DTNB) was used as the chromophoric reagent [29]. Inhibition assays were carried out on an Agilent 8453E UV–visible spectrophotometer equipped with a cell changer. Solutions of tested compounds were prepared starting from 10 mM stock solutions in DMSO, which were diluted with aqueous assay medium to a final content of organic solvent always lower than 1%. AChE inhibitory activity was determined in a reaction mixture containing 100 μL of a solution of AChE (0.9 U/mL in 0.1 M phosphate buffer, pH 8.0), 100 μL of a 3.3 mM solution of DTNB in 0.1 M phosphate buffer (pH 7.0) containing 6 mM $NaHCO_3$, 100 μL of a solution of the inhibitor (six to seven concentrations ranging from $1 \times \cdot 10^{-8}$ to $1 \times \cdot 10^{-4}$ M), and 600 μL of work buffer. After incubation for 20 min at 25 °C, acetylthiocholine iodide (100 μL of 5 mM aqueous solution) was added as the substrate, and AChE-catalyzed hydrolysis was followed by measuring the increase of absorbance at 412 nm for 5.0 min at 25 °C. The concentration of compound which determined 50% inhibition of the AChE activity (IC_{50}) was calculated by nonlinear regression of the response/log(concentration) curve, using GraphPad Prism, version 5. BChE inhibitory activity was assessed similarly using butyrylthiocholine iodide as the substrate.

8.7. TEM studies

Samples for TEM analysis were prepared in PBS with 10% ethanol as co-solvent and incubated for up to 10 days at 37 °C. Final

concentration of $A\beta_{1-40}$ was 50 μM, while compounds **24** and **29** were tested at their maximum of solubility (10 and 50 μM, respectively). A control sample of self-aggregating Aβ was prepared in the same buffer/cosolvent conditions. For each sample, a little drop (20 μL) of incubated sample solution was applied to carbon coated copper/rhodium grid (400 mesh; TAAB Laboratories Equipment Ltd, Aldermaston, Berks, GB). The coated grid was floated for 2 min on the sample drop and rinsed with 200 μL of double distilled water. Negative staining was performed with 200 μL of 2% w/v uranyl acetate solution (TAAB Laboratories Equipment Ltd). After draining off the excess of staining solution by means of a filter paper, the specimen was transferred for examination in a Philips Morgagni 282D transmission electron microscope, operating at 60 kV. Electron micrographs of negatively stained samples were photographed on Kodak electron microscope film 4489 (Kodak Company, New York, USA).

8.8. CD spectroscopic analysis

CD spectra were recorded in the spectral range 195–250 nm, by using 0.1 cm path length quartz cells (280 μL internal volume, from Hellma GmbH & Co KG, Milan, I) with a CD Jasco J-810 single beam spectropolarimeter. Control Aβ and Aβ/inhibitor coincubation samples were the same as in TEM studies. CD spectra were recorded at room temperature at 0.1 nm intervals with 4 nm bandwidth and 100 nm/min scan speed. The baseline was recorded with the buffer/ethanol blank or, for co-incubation experiments, with buffer/ethanol solution of inhibitor blank, and subtracted from corresponding spectra. To follow conformational changes and for inhibition studies, the absolute value of CD signal at 215 nm was plotted *vs.* time of incubation (Fig. 1).

Acknowledgments

The authors wish to thank the Cyprus Research Promotion Foundation [Grants: NEAYPODOMH/NEKYP/0308/02 and YGEIA/BIOS/0308(BIE)/13], the University of Cyprus (Medium Sized Grant), and the following organizations in Cyprus for generous donations of chemicals and glassware: the State General Laboratory, the Agricultural Research Institute, the Ministry of Agriculture, Medochemie Ltd and Biotronics Ltd. Furthermore, we thank the A.G. Leventis Foundation for helping to establish the NMR facility in the University of Cyprus.

This work was also supported by a grant from MIUR (Rome, Italy; PRIN project 20085HR5JK_005).

References

[1] R. Luengo-Fernandez, J. Leal, A.M. Gray, J. Alzheimer's Dis. 27 (2011) 187–196.
[2] A. Wimo, L. Jönsson, A. Gustavsson, D. McDaid, K. Ersek, J. Georges, L. Gulácsi, K. Karpati, P. Kenigsberg, H. Valtonen, Int. J. Geriatr. Psychiatry 26 (2011) 825–832.
[3] H.W. Querfurth, F.M. LaFerla, N. Engl. J. Med. 362 (2010) 329–344.
[4] P.V. Moulton, W. Yang, J. Environ. Public Health (2012) 472751.
[5] L. Bertram, R.E. Tanzi, Prog. Mol. Biol. Transl. Sci. 107 (2012) 79–100.
[6] A. Martorana, Z. Esposito, G. Koch, CNS Neurosci. Ther. 16 (2010) 235–245.
[7] J.C. Rochet, P.T. Lansbury, Curr. Opin. Struct. Biol. 10 (2000) 60–68.
[8] D.M. Walsh, I. Klyubin, J.V. Fadeeva, M.J. Rowan, D.J. Selkoe, Biochem. Soc. Trans. 30 (2002) 552–557.
[9] K. Ono, M. Yamada, J. Neurochem. 117 (2011) 19–28.
[10] F. Chiti, C.M. Dobson, Annu. Rev. Biochem. 75 (2006) 333–366.
[11] M.N. Sabbagh, Am. J. Geriatr. Pharmacother. 7 (2009) 167–185.
[12] M. Bartolini, V. Andrisano, ChemBioChem 11 (2010) 1018–1035.
[13] A.S. DeToma, S. Salamekh, A. Ramamoorthy, M.H. Lim, Chem. Soc. Rev. 41 (2012) 608–621.
[14] S. Cellamare, A. Stefanachi, D.A. Stolfa, T. Basile, M. Catto, F. Campagna, E. Sotelo, P. Acquafredda, A. Carotti, Bioorg. Med. Chem. 16 (2008) 4810–4822.
[15] M. Catto, R. Aliano, A. Carotti, S. Cellamare, F. Palluotto, R. Purgatorio, A. De Stradis, F. Campagna, Eur. J. Med. Chem. 45 (2010) 1359–1366.
[16] F. Campagna, M. Catto, R. Purgatorio, C.D. Altomare, A. Carotti, A. De Stradis, G. Palazzo, Eur. J. Med. Chem. 46 (2011) 275–284.
[17] Proceedings of XXIV National Congress of Italian Chemical Society, Lecce (I), 2011 Sept. 11–16, FAR-PL-04, 340-341.
[18] (a) R. Colombo, E.De Lorenzi, A. Carotti, M. Catto, M. Racchi, C. Lanni, L. Verga, G.Caccialanza, Patent MI2008A366 (2008);
(b) R. Colombo, A. Carotti, M. Catto, M. Racchi, C. Lanni, L. Verga, G. Caccialanza, E. De Lorenzi, Electrophoresis 30 (2009) 1418–1429.
[19] M. Convertino, R. Pellarin, M. Catto, A. Carotti, A. Caflisch, Protein Sci. 18 (2009) 792–800.
[20] (a) A. Carotti, M. De Candia, M. Catto, T.N. Borisova, A.V. Varlamov, E. Méndez-Álvarez, R. Soto-Otero, L.G. Voskressensky, C. Altomare, Bioorg. Med. Chem. 14 (2006) 7205–7212;
(b) F. Leonetti, M. Catto, O. Nicolotti, L. Pisani, A. Cappa, A. Stefanachi, A. Carotti, Bioorg. Med. Chem. 16 (2008) 7450–7456;
(c) L. Pisani, M. Catto, I. Giangreco, F. Leonetti, O. Nicolotti, A. Stefanachi, S. Cellamare, A. Carotti, Chem. Med. Chem. 5 (2010) 1616–1630;
(d) B. Tasso, M. Catto, O. Nicolotti, F. Novelli, M. Tonelli, I. Giangreco, L. Pisani, A. Sparatore, V. Boido, A. Carotti, F. Sparatore, Eur. J. Med. Chem. 46 (2011) 2170–2184;
(e) A. Conejo-García, L. Pisani, M. del Carmen Núñez, M. Catto, O. Nicolotti, F. Leonetti, J. Campos, M. Gallo, A. Espinosa, A. Carotti, J. Med. Chem. 54 (2011) 2627–2645.
[21] P.A. Koutentis, H. Krassos, D. Lo Re, Org. Biomol. Chem. 9 (2011) 5228–5237.
[22] P.A. Koutentis, G. Loizou, D. Lo Re, J. Org. Chem. 76 (2011) 5793–5802.
[23] T.A. Ioannou, P.A. Koutentis, H. Krassos, G. Loizou, D. Lo Re, Org. Biomol. Chem. 10 (2012) 1339–1348.
[24] H.A. Ioannidou, A. Martin, A. Gollner, P.A. Koutentis, J. Org. Chem. 76 (2011) 5113–5122.
[25] A. Gollner, P.A. Koutentis, Org. Lett. 12 (2010) 1352–1355.
[26] L. Pisani, M. Catto, F. Leonetti, O. Nicolotti, A. Stefanachi, F. Campagna, A. Carotti, Curr. Med. Chem. 18 (2011) 4568–4587.
[27] A. Rampa, F. Belluti, S. Gobbi, A. Bisi, Curr. Top. Med. Chem. 11 (2011) 2716–2730.
[28] H. LeVine 3rd, Protein Sci. 2 (1993) 404–410.
[29] G.L. Ellman, K.D. Courtney, V. Andres, R.M. Featherstone, Biochem. Pharmacol. 7 (1961) 88–95.
[30] P.A. Koutentis, D. Lo Re, Synthesis (2010) 2075–2079.
[31] N. Dodic, B. Dumaitre, A. Daugan, P. Pianetti, J. Med. Chem. 38 (1995) 2418–2426.
[32] T. Mohamed, P.P. Rao, Curr. Med. Chem. 18 (2011) 4299–4320.
[33] D. Karlsson, A. Fallarero, G. Brunhofer, C. Mayer, O. Prakash, C.G. Mohan, P. Vuorela, T. Erker, Eur. J. Pharm. Sci. 47 (2012) 190–205.
[34] M. Kitazawa, R. Medeiros, F.M. Laferla, Curr. Pharm. Des. 18 (2012) 1131–1147.
[35] F. Meng, P. Marek, K.J. Potter, C.B. Verchere, D.P. Raleigh, Biochemistry 47 (2008) 6016–6024.
[36] K.H. Lim, H.H. Collver, Y.T.H. Le, P. Nagchowdhuri, J.M. Kenney, Biochem. Biophys. Res. Commun. 353 (2007) 443–449.
[37] T. Akaishi, T. Morimoto, M. Shibao, S. Watanabe, K. Sakai-Kato, N. Utsunomiya-Tate, K. Abe, Neurosci. Lett. 444 (2008) 280–285.